Westinghouse Energy Systems

Westinghouse Energy Systems

WESTINGHOUSE CLASS 3

WCAP-12685

ANALYSIS OF CAPSULE U FROM THE COMMONWEALTH EDISON COMPANY BRAIDWOOD UNIT 1 REACTOR VESSEL RADIATION SURVEILLANCE PROGRAM

E. Terek
S. L. Anderson
L. Albertin

August 1990

Work Performed Under Shop Order BMVP-106

Prepared by Westinghouse Electric Corporation
for the Commonwealth Edison Company

Approved by: T. A. Meyer
T. A. Meyer, Manager
Structural Materials and Reliability Technology

WESTINGHOUSE ELECTRIC CORPORATION
Nuclear and Advanced Technology Division
P.O. Box 2728
Pittsburgh, Pennsylvania 15230-2728

PREFACE

This report has been technically reviewed and verified.

	Reviewer	
Sections 1 through 5, 7, and 8	N. K. Ray	
Section 6	E. P. Lippincott	

TABLE OF CONTENTS

Section	Title	Page
1.0	SUMMARY OF RESULTS	1-1
2.0	INTRODUCTION	2-1
3.0	BACKGROUND	3-1
4.0	DESCRIPTION OF PROGRAM	4-1
5.0	TESTING OF SPECIMENS FROM CAPSULE U	5-1
	5.1 Overview	5-1
	5.2 Charpy V-Notch Impact Test Results	5-3
	5.3 Tension Test Results	5-6
	5.4 Compact Tension Tests	5-6
6.0	RADIATION ANALYSIS AND NEUTRON DOSIMETRY	6-1
	6.1 Introduction	6-1
	6.2 Discrete Ordinates Analysis	6-2
	6.3 Neutron Dosimetry	6-7
7.0	SURVEILLANCE CAPSULE REMOVAL SCHEDULE	7-1
8.0	REFERENCES	8-1

LIST OF ILLUSTRATIONS

Figure	Title	Page
4-1	Arrangement of Surveillance Capsules in the Braidwood Unit 1 Reactor Vessel	4-6
4-2	Capsule U Diagram showing location of specimens, Thermal Monitors and Dosimeters	4-7
5-1	Charpy V-Notch Impact Properties for Braidwood Unit 1 Reactor Vessel Shell Forging 49D867-1/49C813-1 (Tangential Orientation)	5-14
5-2	Charpy V-Notch Impact Properties for Braidwood Unit 1 Reactor Vessel Shell Forging 49D867-1/49C813-1 (Axial Orientation)	5-15
5-3	Charpy V-Notch Impact Properties for Braidwood Unit 1 Reactor Vessel Weld Metal	5-16
5-4	Charpy V-Notch Impact Properties for Braidwood Unit 1 Reactor Weld Heat Affected Zone Metal	5-17
5-5	Charpy Impact Specimen Fracture Surfaces for Braidwood Unit 1 Reactor Vessel Shell Forging 49D867-1/49C813-1 (Tangential Orientation)	5-18
5-6	Charpy Impact Specimen Fracture Surfaces for Braidwood Unit 1 Reactor Vessel Shell Forging 49D867-1/49C813-1 (Axial Orientation)	5-19
5-7	Charpy Impact Specimen Fracture Surfaces for Braidwood Unit 1 Reactor Vessel Weld Metal	5-20
5-8	Charpy Impact Specimen Fracture Surfaces for Braidwood Unit 1 Reactor Vessel Weld Heat Affected Zone (HAZ) Metal	5-21

Figure	Title	Page
5-9	Photographs of Capsule U Specimens (a) ET11 and (b) ET14	5-22
5-10	(a) Photograph of Capsule U Specimen EH2, and (b) Photograph of Capsule U Specimen EW14	5-23
5-11	Tensile Properties for Braidwood Unit 1 Reactor Vessel Shell Forging 49D867-1/49C813-1 (Tangential Orientation)	5-24
5-12	Tensile Properties for Braidwood Unit 1 Reactor Vessel Shell Forging 49D867-1/49C813-1 (Axial Orientation)	5-25
5-13	Tensile Properties for Braidwood Unit 1 Reactor Vessel Weld Metal	5-26
5-14	Fractured Tensile Specimens from Braidwood Unit 1 Reactor Vessel Shell Forging 49D867-1/49C813-1 (Tangential Orientation)	5-27
5-15	Fractured Tensile Specimens from Braidwood Unit 1 Reactor Vessel Shell Forging 49D867-1/49C813-1 (Axial Orientation)	5-28
5-16	Fractured Tensile Specimens from Braidwood Unit 1 Reactor Vessel Weld Metal	5-29
5-17	Typical Stress-Strain Curve for Braidwood Unit 1 Shell Forging 49D867-1/49C813-1 Tension Specimens	5-30
6-1	Plan View of a Dual Reactor Vessel Surveillance Capsule	6-13
6-2	Core Power Distributions used in Transport Calculations for Braidwood Unit 1	6-14

LIST OF TABLES

Table	Title	Page
4-1	Chemical Composition and Heat Treatment of the Braidwood Unit 1 Reactor Vessel Surveillance Materials	4-3
4-2	Chemical Composition of Braidwood Unit 1 Capsule U Irradiated Charpy Impact Specimens	4-4
4-3	Chemistry Results from the NBS Certified Reference Standards	4-5
5-1	Charpy V-Notch Impact Data for the Braidwood Unit 1 Forging 49D867-1/49C813-1 Irradiated at 550°F, Fluence 3.79 x 10^{18} n/cm^2 (E > 1.0 MeV)	5-7
5-2	Charpy V-Notch Impact Data for the Braidwood Unit 1 Reactor Vessel Weld Metal and HAZ Metal Irradiated at 550°F, Fluence 3.79 x 10^{18} n/cm^2 (E > 1.0 MeV)	5-8
5-3	Instrumented Charpy Impact Test Results for the Braidwood Unit 1 Shell Forging 49D867-1/49C813-1 Irradiated at 550°F, Fluence 3.79 x 10^{18} n/cm^2 (E > 1.0 MeV)	5-9
5-4	Instrumented Charpy Impact Test Results for the Braidwood Unit 1 Weld Metal and HAZ Metal Irradiated at 550°F, Fluence 3.79 x 10^{18} n/cm^2 (E > 1.0 MeV)	5-10
5-5	Effect of Irradiation to 3.79 x 10^{18} n/cm^2 (E > 1.0 MeV) at 550°F on Notch Toughness Properties of Braidwood Unit 1 Reactor Vessel Surveillance Materials	5-11

LIST OF TABLES (Cont)

Table	Title	Page
5-6	Comparison of Braidwood Unit 1 Surveillance Material 30 ft-lb Transition Temperature Shifts and Upper Shelf Energy Decreases with Regulatory Guide 1.99 Revision 2 Predictions	5-12
5-7	Tensile Properties for Braidwood Unit 1 Reactor Vessel Surveillance Material Irradiated at 550°F to 3.79×10^{18} n/cm^2 ($E > 1.0$ MeV)	5-13
6-1	Calculated Fast Neutron Exposure Parameters at the Surveillance Capsule Center	6-15
6-2	Calculated Fast Neutron Exposure Parameters at the Pressure Vessel Clad/Base Metal Interface	6-16
6-3	Relative Radial Distributions of Neutron Flux ($E > 1.0$ MeV) within the Pressure Vessel Wall	6-17
6-4	Relative Radial Distributions of Neutron Flux ($E > 1.0$ MeV) within the Pressure Vessel Wall	6-18
6-5	Relative Radial Distributions of Iron Displacement Rate (dpa) within the Pressure Vessel Wall	6-19
6-6	Nuclear Parameters for Neutron Flux Monitors	6-20
6-7	Irradiation History of Neutron Sensors Contained in Capsule U	6-21
6-8	Measured Sensor Activities and Reaction Rates	6-22
6-9	Summary of Neutron Dosimetry Results	6-24

LIST OF TABLES (Cont)

Table	Title	Page
6-10	Comparison of Measured and Ferret Calculated Reaction Rates at the Surveillance Capsule Center	6-25
6-11	Adjusted Neutron Energy Spectrum at the Surveillance Capsule Center	6-26
6-12	Comparison of Calculated and Measured Exposure Levels for Capsule U	6-27
6-13	Neutron Exposure Projections at Key Locations on the Pressure Vessel Clad/Base Metal Interface for Braidwood Unit 1	6-28
6-14	Neutron Exposure Values for use in the Generation of Heatup/Cooldown Curves	6-29
6-15	Updated Lead Factors for Braidwood Unit 1 Surveillance Capsules	6-30

SECTION 1.0
SUMMARY OF RESULTS

The analysis of the reactor vessel material contained in surveillance Capsule U, the first capsule to be removed from the Commonwealth Edison Company Braidwood Unit 1 reactor pressure vessel, led to the following conclusions:

- The capsule received an average fast neutron fluence ($E > 1.0$ MeV) of 3.79×10^{18} n/cm^2 after 1.10 EFPY of plant operation.

- Irradiation of the reactor vessel lower shell forging 49D867-1/49C813-1 Charpy specimens to 3.79×10^{18} n/cm^2 ($E > 1.0$ MeV) resulted in a 30 and 50 ft-lb transition temperature increase of 5 and 10°F, respectively, for specimens oriented parallel to the major working direction (tangential orientation) and no transition temperature increase for specimens oriented normal to the major working direction (axial orientation).

- The weld metal Charpy specimens irradiated to 3.79×10^{18} n/cm^2 ($E > 1.0$ MeV) resulted in a 30 and 50 ft-lb transition temperature increase of 10°F. This results in a 30 ft-lb transition temperature of -10°F and a 50 ft-lb transition temperature of 35°F for the weld metal.

- Irradiation of the reactor vessel weld HAZ metal Charpy specimens to 3.79×10^{18} n/cm^2 resulted in a 30 ft-lb transition temperature increase of 20°F and a 50 ft-lb transition temperature increase of 35°F.

- The average upper shelf energy of the lower shell forging 49D867-1/49C813-1 showed no decrease in energy after irradiation to 3.79×10^{18} n/cm^2 for specimens oriented parallel to the major working direction (tangential orientation) and a decrease of 14 ft-lb for specimens oriented normal to the major working direction (axial orientation). The weld metal showed no decrease in upper

shelf energy after irradiation to 3.79×10^{18} n/cm^2 . Both materials exhibit a more than adequate upper shelf energy level for continued safe plant operation and are expected to maintain an upper shelf energy of no less than 50 lb-ft throughout the life of the vessel as required by 10CFR50, Appendix G.

- The surveillance capsule test results do not indicate any significant changes in the RT_{NDT} values of the reactor vessel surveillance material.

- The calculated end-of-life (32 EFPY) maximum neutron fluence (E > 1.0 MeV) for the Braidwood Unit 1 reactor vessel clad/base metal interface is as follows:

  Vessel inner radius - 3.03×10^{19} n/cm^2
  Vessel 1/4 thickness - 1.66×10^{19} n/cm^2
  Vessel 3/4 thickness - 3.57×10^{18} n/cm^2

  The end-of-life (32 EFPY) maximum neutron fluence values presented above are expected to drop with the implementation of a low leakage fuel management program.

SECTION 2.0
INTRODUCTION

This report presents the results of the examination of Capsule U, the first capsule to be removed from the reactor in the continuing surveillance program which monitors the effects of neutron irradiation on the Braidwood Unit 1 reactor pressure vessel materials under actual operating conditions.

The surveillance program for the Braidwood Unit 1 reactor pressure vessel materials was designed and recommended by the Westinghouse Electric Corporation. A description of the surveillance program and the preirradiation mechanical properties of the reactor vessel materials are presented in WCAP-9807 "Commonwealth Edison Company Braidwood Station Unit No. 1, Reactor Vessel Radiation Surveillance Program" by Yanichko and Singer.[1] The surveillance program was planned to cover the 40-year design life of the reactor pressure vessel and was based on ASTM E-185-73, "Standard Recommended Practice for Surveillance Tests for Nuclear Reactor Vessels". Westinghouse Power Systems personnel were contracted to aid in the preparation of procedures for removing capsule "U" from the reactor and its shipment to the Westinghouse Science and Technology Center where the postirradiation mechanical testing of the Charpy V-notch impact and tensile surveillance specimens was performed at the Westinghouse Science and Technology Center Hot Cell.

This report summarizes the testing of and the postirradiation data obtained from surveillance Capsule "U" removed from the Braidwood Unit 1 reactor vessel and discusses the analysis of these data.

SECTION 3.0
BACKGROUND

The ability of the large steel pressure vessel containing the reactor core and its primary coolant to resist fracture constitutes an important factor in ensuring safety in the nuclear industry. The beltline region of the reactor pressure vessel is the most critical region of the vessel because it is subjected to significant fast neutron bombardment. The overall effects of fast neutron irradiation on the mechanical properties of low alloy, ferritic pressure vessel steels such as SA 508 Class 3 (base material of the Commonwealth Edison Company Station Braidwood Unit 1 reactor pressure vessel lower shell forging) are well documented in the literature. Generally, low alloy ferritic materials show an increase in hardness and tensile properties and a decrease in ductility and toughness under certain conditions of irradiation.

A method for performing analyses to guard against fast fracture in reactor pressure vessels have been presented in "Protection Against Nonductile Failure," Appendix G to Section III of the ASME Boiler and Pressure Vessel Code. The method uses fracture mechanics concepts and is based on the reference nil-ductility temperature (RT_{NDT}).

RT_{NDT} is defined as the greater of either the drop weight nil-ductility transition temperature (NDTT per ASTM E-208) or the temperature 60°F less than the 50 ft-lb (and 35-mil lateral expansion) temperature as determined from Charpy specimens oriented normal (axial) to the major working direction of the material. The RT_{NDT} of a given material is used to index that material to a reference stress intensity factor curve (K_{IR} curve) which appears in Appendix G of the ASME Code. The K_{IR} curve is a lower bound of dynamic, crack arrest, and static fracture toughness results obtained from several heats of pressure vessel steel. When a given material is indexed to the K_{IR} curve, allowable stress intensity factors can be obtained for this material as a function of temperature. Allowable operating limits can then be determined using these allowable stress intensity factors.

RT_{NDT} and, in turn, the operating limits of nuclear power plants can be adjusted to account for the effects of radiation on the reactor vessel material properties. The radiation embrittlement changes in mechanical properties of a given reactor pressure vessel steel can be monitored by a reactor surveillance program such as the Braidwood Unit 1 Reactor Vessel Radiation Surveillance Program,[1] in which a surveillance capsule is periodically removed from the operating nuclear reactor and the encapsulated specimens are tested. The increase in the average Charpy V-notch 30 ft-lb temperature (ΔRT_{NDT}) due to irradiation is added to the original RT_{NDT} to adjust the RT_{NDT} for radiation embrittlement. This adjusted RT_{NDT} (RT_{NDT} initial + ΔRT_{NDT}) is used to index the material to the K_{IR} curve and, in turn, to set operating limits for the nuclear power plant which take into account the effects of irradiation on the reactor vessel materials.

SECTION 4.0
DESCRIPTION OF PROGRAM

Six surveillance capsules for monitoring the effects of neutron exposure on the Braidwood Unit 1 reactor pressure vessel core region material were inserted in the reactor vessel prior to initial plant startup. The six capsules were positioned in the reactor vessel between the neutron shield pads and the vessel wall as shown in Figure 4-1. The vertical center of the capsules is opposite the vertical center of the core.

Capsule U was removed after 1.10 effective full power years of plant operation. This capsule contained Charpy V-notch, tensile, and 1/2 T compact tension (CT) specimens (Figure 4-2) from the lower shell forging 49D867-1/49C813-1 and weld metal representative of the intermediate to lower shell beltline weld seam of the reactor vessel and Charpy V-notch specimens from weld heat-affected zone (HAZ) material. All heat-affected zone specimens were obtained from within the HAZ of forging 49D867-1/49C813-1 of the representative weld.

The chemical composition and heat treatment of the surveillance material is presented in Table 4-1. The chemical analyses reported in Table 4-1 were obtained from unirradiated material used in the surveillance program. In addition, a chemical analysis using Inductively Coupled Plasma Spectrometry (ICPS) was performed on irradiated specimens from forging 49D867-1/49C813-1 and weld metal and is reported in Table 4-2. The chemistry results from the NBS certified reference standards are reported in Table 4-3.

All test specimens were machined from the 1/4 thickness location of the forging. Test specimens represent material taken at least one forging thickness from the quenched end of the forging. Base metal Charpy V-notch impact and tension specimens were oriented with the longitudinal axis of the specimen parallel to the major working direction of the forging (tangential orientation) and also normal to the major working direction (axial orientation). Charpy V-notch and tensile specimens from the weld metal were oriented with the longitudinal axis of the specimens transverse to the welding

direction. The Compact Tension test specimens in Capsule U are from the lower shell course forging and were machined in both tne axial and tangential orientations. Thus, the simulated crack in the specimen will propogate normal and parallel to the major working direction of forging 49D867-1/49C813-1. Compact Tension Test specimens from the weld metal were machined normal to the weld direction with the notch oriented in the direction of the weld. Thus, the simulated crack in the specimen will propogate parallel to the weld direction. All CT specimens were fatigue precracked according to ASTM E399.

Capsule U contained dosimeter wires of pure copper, iron, nickel, and aluminum-0.15% colbalt (cadmium-shielded and unshielded). In addition, cadmium shielded dosimeters of neptunium (Np^{237}) and uranium (U^{238}) were contained in the capsule.

Thermal monitors made from the two low-melting eutectic alloys and sealed in Pyrex tubes were included in the capsule. The composition of the two alloys and their melting points are as follows:

2.5% Ag, 97.5% Pb	Melting Point: 579°F (304°C)
1.75% Ag, 0.75% Sn, 97.5% Pb	Melting Point: 590°F (310°C)

The arrangement of the various mechanical specimens, dosimeters and thermal monitors contained in Capsule U are shown in Figure 4-2.

TABLE 4-1

CHEMICAL COMPOSITION AND HEAT TREATMENT OF THE BRAIDWOOD UNIT 1 REACTOR VESSEL SURVEILLANCE MATERIALS [1]

Element	Chemical Composition (wt%) Lower Shell Forging 49D867-1/49C813-1	Weld Metal
C	.20	.066
Mn	1.33	1.44
P	.007	.015
S	.006	.012
Si	.28	.48
Ni	.73	.67
Mo	.52	.44
Cr	.11	.10
Cu	.03	.04
Al	.018	.004
Co	.011	.011
Pb	.0003	.0006
W	.005	.010
Ti	.005	.007
Zr	.005	.003
V	.01	.005
Sn	.008	.005
As	.008	.004
Cb	.005	.004
N_2	.0096	.013
B	.0001	.0007

HEAT TREATMENT HISTORY

Material	Temperature (°F)	Time (hr)	Cooling
Lower Shell Forging 49D867-1/ 49C813-1	Austenitizing: 1600 - 1652	8½	Water-quenched
	Tempered: 1202 - 1229	7½	Air-cooled
	Stress Relief: 1100 - 1150	12¼	Furnace-cooled
Weldment	1100 - 1150	12¼	Furnace-cooled

TABLE 4-2
CHEMICAL COMPOSITION OF BRAIDWOOD UNIT 1 CAPSULE U IRRADIATED CHARPY IMPACT SPECIMENS

Chemical Composition (wt.%)

Metal	Specimen No. EL-6	EW-4	EW-15	EW-1	EW-2	EW-3	EW-5	EW-6	EW-7	EW-8	EW-9	EW-10	EW-11	EW-12	EW-13	EW-14
Fe	(Matrix Element: Remainder by Difference)															
Mn	1.300	1.470	1.490													
Cr	0.118	0.084	0.086													
Ni	0.746	0.666	0.666	0.723	0.709	0.728	0.699	0.751	0.683	0.673	0.668	0.686	0.616	0.651	0.598	0.656
Mo	0.574	0.444	0.444													
Co	<0.01	<0.01	<0.01													
Cu	0.052	0.035	0.033	0.034	0.035	0.034	0.035	0.035	0.031	0.032	0.029	0.029	0.034	0.033	0.033	0.031
P	<0.01	<0.01	<0.01													
V	<0.01	<0.01	<0.01													
C	0.207	0.065	0.063													
S	0.005	0.013	0.013													
Si	0.298	0.495	0.488													

Analyses	Method of Analysis
Metals	ICPS, Inductively Coupled Plasma Spectrometry
Carbon	EC-12, LECO Carbon Analyzer
Sulfur	Combusion/titration
Silicon	Dissolution/gravimetric

TABLE 4-3
CHEMISTRY RESULTS FROM THE NBS
CERTIFIED REFERENCE STANDARDS

Material ID: Low Alloy Steel: NBS Certified Reference Standards

	NBS 361		NBS 362	
	Certified	Measured (a)	Certified	Measured (a)
Metals	Concentration in Weight Percent			
Fe *	95.60	(matrix)	95.30	(matrix)
Mn	0.660	0.643	1.040	1.010
Cr	0.694	0.668	0.300	0.289
Ni	2.000	2.030	0.590	0.591
Mo	0.190	0.205	0.068	0.064
Co	0.032	0.035	0.300	0.298
Cu	0.042	0.046	0.500	0.505
P	0.014	0.018	0.041	0.039
V	0.011	0.007	0.040	0.044
C	0.383	-----	0.160	0.160/0.159
S	0.014	-----	0.036	0.037
Si	0.222	0.240	0.390	0.397

Material ID: Low Alloy Steel: NBS Certified Reference Standards

	NBS 363	
	Certified	Measured (a)
Metals	Concentration in Weight Percent	
Fe *	94.4[illegible]	NA
Mn	1.500	NA
Cr	1.310	NA
Ni	0.300	0.307
Mo	0.028	NA
Co	0.048	NA
Cu	0.100	0.100
P	0.029	NA
V	0.310	NA
C	0.620	NA
S	0.0068	NA

* Matrix element calculated as difference for material balance.
Tentative value, certified ± 100% of value.
NA - Not analyzed; NR, Not requested

(a) Method of analysis -- Inductively Coupled Plasma Spectrometry (ICPS) for all elements except C, S and Si.

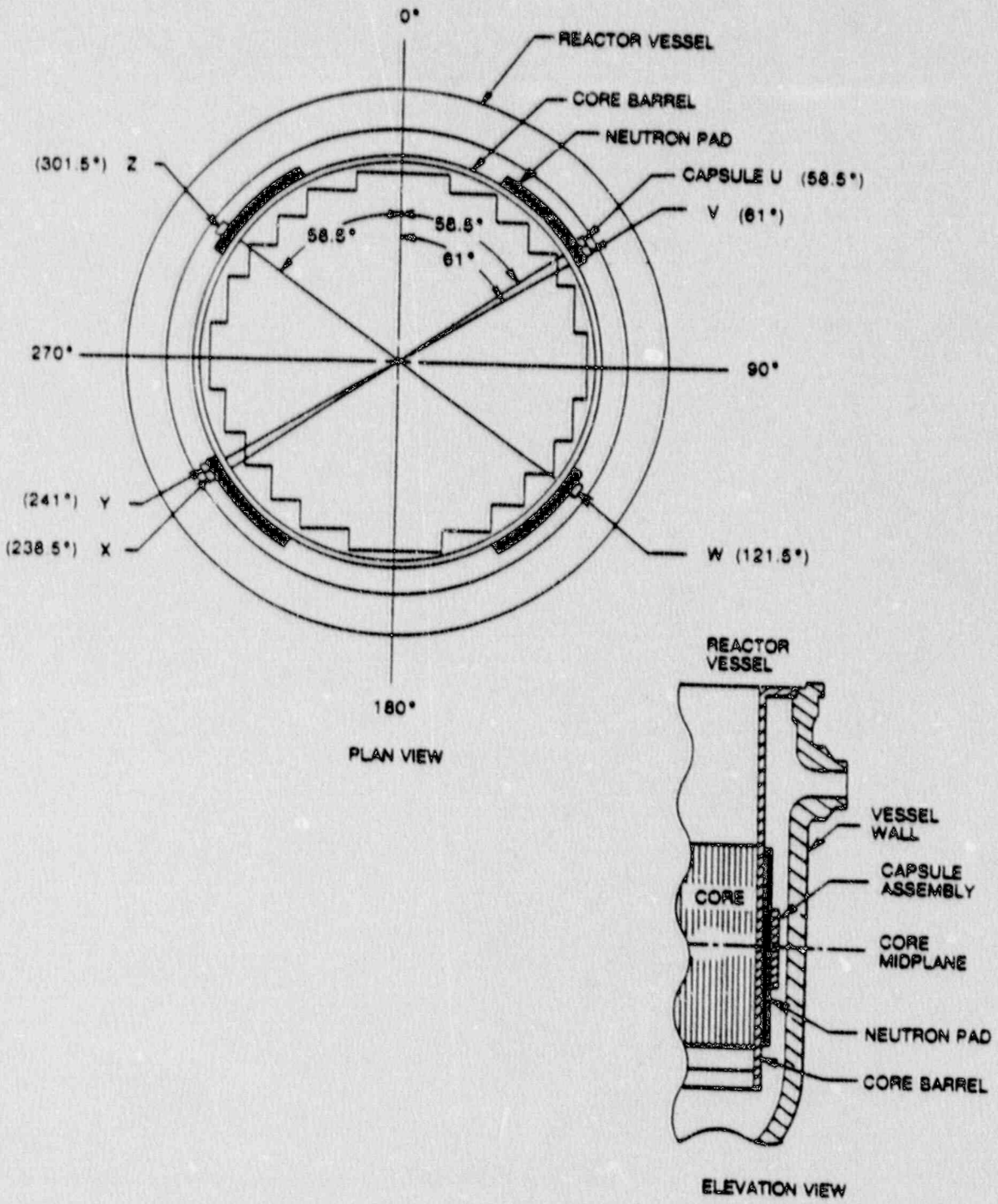

Figure 4-1. Arrangement of Surveillance Capsules in the Braidwood Unit 1 Reactor Vessel

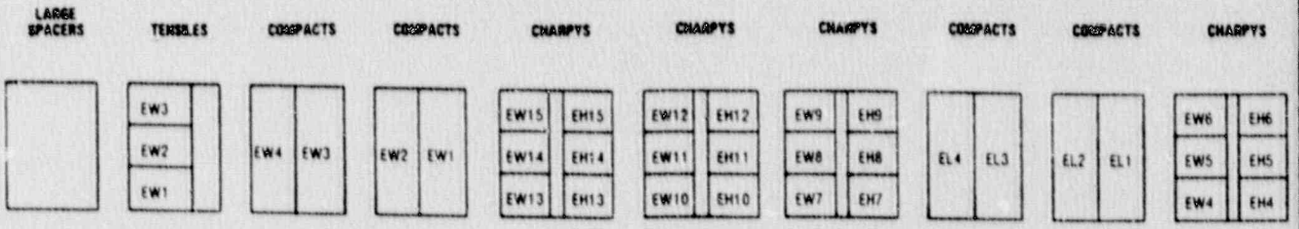

LEGEND: EL - LOWER SHELL FORGING 49D867-1/49C813-1 (TANGENTIAL)
ET - LOWER SHELL FORGING 49D867-1/49C813-1 (AXIAL)
EW - WELD METAL
EH - HEAT-AFFECTED-ZONE MATERIAL

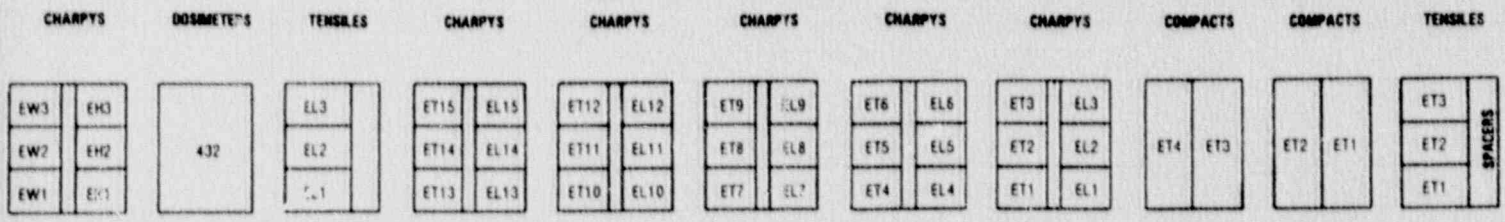

Figure 4-2. Capsule U Diagram Showing Location of Specimens, Thermal Monitors and Dosimeters

SECTION 5.0
TESTING OF SPECIMENS FROM CAPSULE U

5.1 Overview

The post-irradiation mechanical testing of the Charpy V-notch and tensile specimens was performed at the Westinghouse Science and Technology Center with consultation by Westinghouse Power Systems personnel. Testing was performed in accordance with 10CFR50, Appendices G and H,[2] ASTM Specification E185-82[6], and Westinghouse Procedure MHL 8402, Revision 1 as modified by Westinghouse RMF Procedures 8102, Revision 1 and 8103, Revision 1.

Upon receipt of the capsule at the laboratory, the specimens and spacer blocks were carefully removed, inspected for identification number, and checked against the master list in WCAP-9807[1]. No discrepancies were found.

Examination of the two low-melting point 304°C (579°F) and 310°C (590°F) eutectic alloys indicated no melting of either type of thermal monitor. Based on this examination, the maximum temperature to which the test specimens were exposed was less than 304°C (579°F).

The Charpy impact tests were performed per ASTM Specification E23-88[7] and RMF Procedure 8103, Revision 1 on a Tinius-Olsen Model 74,358J machine. The tup (striker) of the Charpy machine is instrumented with an Effects Technology Model 500 instrumentation system. With this system, load-time and energy-time signals can be recorded in addition to the standard measurement of Charpy energy (E_D). From the load-time curve, the load of general yielding (P_{GY}), the time to general yielding (t_{GY}), the maximum load (P_M), and the time to maximum load (t_M) can be determined. Under some test conditions, a sharp drop in load indicative of fast fracture was observed. The load at which fast fracture was initiated is identified as the fast fracture load (P_F), and the load at which fast fracture terminated is identified as the arrest load (P_A).

The energy at maximum load (E_M) was determined by comparing the energy-time record and the load-time record. The energy at maximum load is roughly equivalent to the energy required to initiate a crack in the specimen. Therefore, the propagation energy for the crack (E_p) is the difference between the total energy to fracture (E_D) and the energy at maximum load.

The yield stress (σ_Y) is calculated from the three-point bend formula. The flow stress is calculated from the average of the yield and maximum loads, also using the three-point bend formula.

Percent shear was determined from post-fracture photographs using the ratio-of-areas methods in compliance with ASTM Specification A370-89[8]. The lateral expansion was measured using a dial gage rig similar to that shown in the same specification.

Tension tests were performed on a 20,000-pound Instron, split-console test machine (Model 1115) per ASTM Specification E8-89[9] and E21-79 (1988)[10], and RMF Procedure 8102, Revision 1. All pull rods, grips, and pins were made of Inconel 718 hardened to HRC45. The upper pull rod was connected through a universal joint to improve axiality of loading. The tests were conducted at a constant crosshead speed of 0.05 inches per minute throughout the test.

Deflection measurements were made with a linear variable displacement transducer (LVDT) extensometer. The extensometer knife edges were spring-loaded to the specimen and operated through specimen failure. The extensometer gage length is 1.00 inch. The extensometer is rated as Class B-2 per ASTM E83-85[11].

Elevated test temperatures were obtained with a three-zone electric resistance split-tube furnace with a 9-inch hot zone. All tests were conducted in air.

Because of the difficulty in remotely attaching a thermocouple directly to the specimen, the following procedure was used to monitor specimen temperature: Chromel-alumel thermocouples were inserted in shallow holes in the center and

each end of the gage section of a dummy specimen and in each grip. In the test configuration, with a slight load on the specimen, a plot of specimen temperature versus upper and lower grip and controller temperatures was developed over the range of room temperature to 550°F (288°C). The upper grip was used to control the furnace temperature. During the actual testing the grip temperatures were used to obtained desired specimen temperatures. Experiments indicated that this method is accurate to ±2°F.

The yield load, ultimate load, fracture load, total elongation, and uniform elongation were determined directly from the load-extension curve. The yield strength, ultimate strength, and fracture strength were calculated using the original cross-sectional area. The final diameter and final gage length were determined from post-fracture photographs. The fracture area used to calculate the fracture stress (true stress at fracture) and percent reduction in area was computed using the final diameter measurement.

5.2 Charpy V-Notch Impact Test Results

The results of Charpy V-notch impact tests performed on the various materials contained in Capsule U irradiated to 3.79×10^{18} n/cm^2 (E > 1.0 MeV) are presented in Tables 5-1 through 5-5 and are compared with unirradiated results[1] in Figures 5-1 through 5-4. The transition temperature increases and upper shelf energy decreases for the Capsule U materials are summarized in Table 5-6.

Irradiation of Charpy specimens oriented with the longitudinal axis of the specimen parallel to the major working direction (tangential orientation) of the reactor vessel lower shell forging 50D102-1/50D97-1 to 3.79×10^{18} n/cm^2 (E > 1.0 MeV) at 500°F (Figure 5-1) resulted in the following; a 30 ft-lb transition temperature increase of 5°F which results in a 30 ft-lb transition temperature of -60°F and a 50 ft-lb transition temperature increase of 10°F which results in a 50 ft-lb transition temperature of -30°F.

The average upper shell energy (USE) of Charpy specimens oriented with the longitudinal axis of the specimen parallel to the major working direction (tangential orientation) of the lower shell forging 50D102-1/50D97-1 resulted in no energy decrease after irradiation to 3.79×10^{18} n/cm^2 (E > 1.0 MeV) at 550°F. This results in an average USE of 168 ft-lb (Figure 5-1).

Irradiation of Charpy specimens oriented with the longitudinal axis of the specimen normal to the major working direction (axial orientation) of the reactor vessel lower shell forging 50D102-1/50D97-1 to 3.79×10^{18} n/cm^2 (E > 1.0 MeV) at 550°F (Figure 5-2) resulted in no 30 and 50 ft-lb transition temperature increases. This results in a 30 ft-lb transition temperature of -45°F and a 50 ft-lb transition temperature of -15°F.

The average upper shelf energy (USE) of Charpy specimens oriented with the longitudinal axis of the specimen normal to the major working direction (axial orientation) of the lower shell forging 50D102-1/50D97-1 resulted in an average USE decrease of 14 ft-lb after irradiation to 3.79×10^{18} n/cm^2 (E > 1.0 MeV) at 550°F. This results in an USE of 138 ft-lb (Figure 5-2).

Irradiation of the reactor vessel core region weld metal Charpy specimens to 3.79×10^{18} n/cm^2 (E > 1.0 MeV) at 550°F (Figure 5-3) resulted in 30 and 50 ft-lb transition temperature increases of 10°F. This resulted in a 30 ft-lb transition temperature of -10°F and a 50 ft-lb transition temperature of 35°F.

The average upper shelf energy (USE) of the reactor vessel core region weld metal Charpy specimens resulted in no energy decrease after irradiation to 3.79×10^{18} n/cm^2 (E > 1.0 MeV) at 550°F. This resulted in an average USE of 70 ft-lb (Figure 5-3).

Irradiation of the reactor vessel weld metal Heat-Affected Zone (HAZ) Charpy specimens to 3.79×10^{18} n/cm^2 (E > 1.0 MeV) at 550°F (Figure 5-4) resulted in 30 ft-lb transition temperature increase of 20°F which results in a 30 ft-lb transition temperature of -150°F and a 50 ft-lb transition temperature increases of 35°F which results in a 50 ft-lb transition temperature of 105°F.

The average upper shelf energy (USE) of the reactor vessel HAZ metal Charpy specimens resulted in an increase of 3 ft-lb after irradiation to 3.79 x 10^{18} n/cm^2 (E > 1.0 MeV) at 550°F. This resulted in an average USE of 112 ft-lb.

The fracture appearance of each irradiated Charpy specimen from the various materials is shown in Figures 5-5 through 5-8 and show an increasingly ductile or tougher appearance with increasing test temperature.

A comparison of the 30 ft-lb transition temperature increases and the upper shelf energy decreases for the various Braidwood Unit 1 surveillance materials with predictions using the methods of NRC Regulatory Guide 1.99, Revision 2[3] is presented in Table 5-6. This comparison indicates that the transition temperature increases and the upper shelf energy decreases resulting from irradiation to 3.79 x 10^{18} n/cm^2 are less than the Guide predictions.

During the testing of the Braidwood Unit 1 surveillance capsule U Charpy specimens the machine loader malfunctioned. This resulted in two of the Charpy specimens, ET14 and ET11, to be improperly tested. Figure 5-9 provides photographs of the specimens that were affected. During the loading of these two specimens, the loading device flipped the specimens such that the hammer struck 90° to the notched surface. The cause of the malfunction is believed to be associated with excursions in pneumatic pressure of the loading device. The loader was repaired and tested. The specimens tested prior to and following the malfunction were carefully examined to insure that they had been properly loaded.

Figure 5-10 (a) is a photograph of HAZ metal specimen EH-2, which failed at a high energy level. The large branching cracks at the root of the notch verify that the specimen was very tough. The darker side of the specimen is base metal and the lighter side of the specimen is weld metal. It appears that the notch was placed in the base metal and that the fracture proceeded through the base except for the final 1/3 of the specimen which would be a small part of the energy absorbed. It is difficult to reconstruct the exact shape of the weld/base metal interface because of the deformation incurred during the

test. However, it appears that there may have been a protrusion where the specimen was cut. The expected weld/base metal interface is shown in Figure 5-10 (b) for comparison purposes.

5.3 Tension Test Results

The results of tension tests performed on shell forging 49D867-1/49D813-1 (tangential and axial orientation) and the weld metal irradiated to 3.79 x 10^{18} n/cm^2 are shown in Table 5-7 and are compared with unirradiated results[1] as shown in Figures 5-9, 5-10 and 5-11. Forging 49D867-1/49D813-1 test results are shown in Figures 5-9 and 5-10 and indicated that irradiation to 3.79 x 10^{18} n/cm^2 caused a less than 8 ksi increase in the 0.2 percent offset yield strength and ultimate tensile strength. Weld metal tension tests results shown in Figure 5-11, show that the ultimate tensile strength and the 0.2 percent offset yield strength increased by less then 10 ksi with irradiation. The small increases in 0.2% yield strength and tensile strength exhibited by the forging material and weld metal indicate that these materials are not highly sensitive to radiation at 3.79 x 10^{18} n/cm^2, as is also indicated by the Charpy impact test results. The fractured tension specimens for the forging material are shown in Figures 5-12 and 5-13, while the fractured specimens for the weld metal are shown in Figure 5-14. A typical stress-strain curve for the tension tests is shown in Figure 5-15.

5.4 Compact Tension Tests

Per the surveillance capsule testing program with the Commonwealth Edison Company, 1/2 T-compact tension fracture mechanics specimens will not be tested and will be stored at the Westinghouse Science and Technology Center Hot Cell.

TABLE 5-1

CHARPY V-NOTCH IMPACT DATA FOR THE BRAIDWOOD UNIT 1

FORGING 49D867-1/49D813-1 IRRADIATED AT 550°F,

FLUENCE 3.79 x 10^{18} n/cm^2 (E > 1.0 MeV)

Sample No.	Temperature (°F)	(°C)	Impact Energy (ft-lb)	(J)	Lateral Expansion (mils)	(mm)	Shear (%)
			Tangential Orientation				
EL13	-150	(-101)	12.0	(16.5)	10.0	(0.25)	10
EL15	-100	(-73)	23.0	(31.0)	16.0	(0.41)	15
EL4	-85	(-65)	18.0	(24.5)	20.0	(0.51)	15
EL9	-50	(-46)	11.0	(15.0)	9.0	(0.23)	10
EL5	0	(-18)	79.0	(107.0)	55.0	(1.40)	50
EL1	0	(-18)	116.0	(157.5)	68.0	(1.73)	65
EL12	25	(- 4)	130.0	(176.5)	73.0	(1.85)	80
EL7	50	(10)	113.0	(153.0)	67.0	(1.70)	75
EL14	50	(10)	124.0	(168.0)	72.0	(1.83)	90
EL6	100	(38)	122.0	(165.5)	71.0	(1.80)	85
EL3	150	(66)	162.0	(219.5)	87.0	(2.21)	100
EL2	150	(66)	163.0	(221.0)	89.0	(2.26)	100
EL10	200	(93)	171.0	(232.0)	87.0	(2.21)	100
EL11	200	(93)	172.0	(233.0)	88.0	(2.21)	100
EL8	250	(121)	174.0	(236.5)	86.0	(2.18)	100
			Axial Orientation				
ET14	-125	(-87)	BAD TEST (MACHINE MALFUNCTION)				
ET10	- 80	(-62)	19.0	(26.0)	13.0	(0.33)	15
ET1	- 80	(-62)	42.0	(57.0)	27.0	(0.69)	25
ET3	- 50	(-46)	24.0	(32.5)	15.0	(0.38)	20
ET2	- 50	(-46)	34.0	(46.0)	31.0	(0.79)	25
ET9	- 20	(-29)	50.0	(68.5)	32.0	(0.81)	25
ET12	0	(-18)	75.0	(101.5)	51.0	(1.30)	45
ET11	25	(- 4)	BAD TEST (MACHINE MALFUNCTION)				
ET6	50	(10)	98.0	(133.0)	63.0	(1.60)	75
ET5	50	(10)	102.0	(138.5)	64.0	(1.63)	80
ET4	100	(38)	104.0	(141.0)	69.0	(1.75)	90
ET8	150	(66)	135.0	(183.0)	84.0	(2.13)	100
ET7	150	(66)	142.0	(192.5)	84.0	(2.13)	100
ET13	200	(93)	136.0	(184.5)	85.0	(2.16)	100
ET15	225	(107)	136.0	(184.5)	75.0	(1.91)	100

TABLE 5-2

CHARPY V-NOTCH IMPACT DATA FOR THE BRAIDWOOD UNIT 1 REACTOR VESSEL WELD METAL AND HAZ METAL IRRADIATED AT 550°F, FLUENCE 3.79 x 10^{18} n/cm^2 (E > 1.0 MeV)

Sample No.	Temperature (°F)	(°C)	Impact Energy (ft-lb)	(J)	Lateral Expansion (mils)	(mm)	Shear (%)
			Weld Metal				
EW4	-55	(-48)	16.0	(21.5)	14.0	(0.36)	10
EW14	-25	(-32)	14.0	(19.0)	13.0	(0.33)	15
EW13	-10	(-23)	28.0	(38.0)	22.0	(0.56)	20
EW11	-10	(-23)	39.0	(53.0)	31.0	(0.79)	25
EW15	25	(- 4)	43.0	(58.5)	35.0	(0.89)	35
EW6	25	(- 4)	46.0	(62.5)	40.0	(1.02)	35
EW10	75	(24)	64.0	(87.0)	52.0	(1.32)	95
EW1	75	(24)	67.0	(91.0)	55.0	(1.40)	100
EW2	100	(38)	63.0	(85.5)	51.0	(1.30)	100
EW9	100	(38)	73.0	(99.0)	59.0	(1.50)	100
EW12	150	(66)	64.0	(87.0)	51.0	(1.30)	100
EW5	150	(66)	72.0	(97.5)	59.0	(1.50)	100
EW7	175	(79)	69.0	(93.5)	61.0	(1.55)	100
EW3	215	(102)	76.0	(103.0)	61.0	(1.55)	100
EW8	215	(102)	78.0	(106.0)	61.0	(1.55)	100
			HAZ Metal				
EH14	-150	(-101)	23.0	(31.0)	10.0	(0.25)	10
EH3	-150	(-101)	56.0	(76.0)	30.0	(0.76)	25
EH13	-100	(-73)	26.0	(35.5)	20.0	(0.51)	15
EH7	- 50	(-46)	32.0	(43.5)	26.0	(0.66)	20
EH1	- 50	(-46)	85.0	(115.0)	46.0	(1.17)	50
EH8	0	(-18)	78.0	(106.0)	47.0	(1.19)	60
EH2	0	(-18)	144.0	(195.0)	76.0	(1.93)	75
EH4	50	(-10)	72.0	(97.5)	44.0	(1.12)	60
EH10	50	(10)	72.0	(97.5)	44.0	(1.12)	60
EH11	100	(38)	102.0	(138.5)	59.0	(1.50)	95
EH5	100	(38)	116	(157.5)	65.0	(1.65)	95
EH6	175	(79)	94.0	(127.5)	62.0	(1.57)	100
EH9	200	(93)	113.0	(153.0)	77.0	(1.96)	100
EH15	250	(121)	118.0	(160.0)	65.0	(1.65)	100
EH12	250	(121)	126.0	(171.0)	71.0	(1.80)	100

TABLE 5-3

INSTRUMENTED CHARPY IMPACT TEST RESULTS FOR THE BRAIDWOOD UNIT 1

SHELL FORGING 490867-1/490813-1 IRRADIATED AT 550°F, FLUENCE 3.79 x 10^{18} n/cm^2 (E > 1.0 MeV)

Sample Number	Test Temp (°F)	Charpy Energy (ft-lb)	Normalized Energies Charpy Ed/A (ft-lb/in²)	Maximum Em/A (ft-lb/in²)	Prop Ep/A (ft-lb/in²)	Yield Load (kips)	Time to Yield (μsec)	Maximum Load (kips)	Time to Maximum (μsec)	Fracture Load (kips)	Arrest Load (kips)	Yield Stress (ksi)	Flow Stress (ksi)
Tangential Orientation													
EL13	-150	12.0	97	79	18	4.10	120	4.65	210	4.65	-	136	145
EL15	-100	23.0	185	154	31	3.60	75	4.70	330	4.70	-	120	138
EL4	- 85	18.0	145	122	23	2.85	90	4.40	300	4.30	-	93	119
EL9	- 50	11.0	89	64	24	3.35	110	3.80	200	3.80	-	111	119
EL5	0	79.0	636	311	325	3.40	110	4.60	670	4.25	-	113	133
EL1	0	116.0	934	317	617	3.55	110	5.05	630	4.15	1.95	118	143
EL12	25	130.0	1047	396	650	3.90	190	4.85	800	3.75	1.85	128	145
EL7	50	113.0	910	325	585	3.05	165	4.55	745	3.95	1.40	100	126
EL14	50	124.0	998	310	689	3.2	150	4.55	725	3.70	1.75	105	128
EL6	100	122.0	982	377	606	3.15	125	4.45	845	3.70	2.05	104	125
EL3	150	162.0	1304	358	946	2.95	140	4.30	850	-	-	97	119
EL2	150	163.0	1313	316	997	3.15	70	4.70	700	0.35	0.35	103	124
EL10	200	171.0	1377	354	1023	2.75	130	4.20	875	-	-	91	115
EL11	200	172.0	1385	273	1112	2.85	30	4.25	620	0.30	0.30	95	118
EL8	250	174.0	1401	195	1206	1.45	150	2.70	805	-	-	49	69
Axial Orientation													
ET14	-125	BAD TEST (MACHINE MALFUNCTION)				-	-	-	-	-	-	-	-
ET10	- 80	19.0	153	128	25	3.80	120	4.40	310	4.3	-	126	135
ET1	- 80	42.0	338	279	59	3.45	65	4.80	550	4.70	0.15	113	136
ET3	- 50	24.0	193	160	33	2.85	150	4.45	420	4.40	-	95	121
ET2	- 50	34.0	274	242	32	3.60	120	4.70	520	4.65	-	119	137
ET9	- 20	50.0	403	283	120	3.70	140	4.70	625	4.55	0.25	123	139
ET12	0	75.0	604	333	271	3.55	190	4.70	730	4.25	0.30	117	136
ET11	25	BAD TEST (MACHINE MALFUNCTION)				-	-	-	-	-	-	-	-
ET6	50	98.0	786	324	465	2.85	145	4.55	730	3.75	1.15	94	123
ET5	50	102.0	821	304	517	3.25	150	4.50	695	3.60	0.90	108	129
ET4	100	104.0	837	294	543	3.10	120	4.30	690	3.60	2.25	102	122
ET8	150	135.0	1087	321	766	3.00	130	4.20	765	-	-	99	119
ET7	150	142.0	1143	324	820	2.7	135	4.30	805	-	-	88	116
ET13	200	136.0	1095	322	773	2.85	175	4.25	805	-	-	94	117
ET15	225	136.0	1095	316	779	2.80	125	4.00	785	-	-	92	112

TABLE 5-4

INSTRUMENTED CHARPY IMPACT TEST RESULTS FOR THE BRAIDWOOD UNIT 1

WELD METAL AND HAZ METAL IRRADIATED AT 550°F, FLUENCE 3.79 x 10^{18} n/cm^2 (E > 1.0 MeV)

Sample Number	Test Temp (°F)	Charpy Energy (ft-lb)	Normalized Energies (ft-lb/in^2) Charpy Ed/A	Maximum Em/A	Prop Ep/A	Yield Load (kips)	Time to Yield (μsec)	Maximum Load (kips)	Time to Maximum (μsec)	Fracture Load (kips)	Arrest Load (kips)	Yield Stress (ksi)	Flow Stress (ksi)
							Weld Metal						
EW4	-55	16.0	129	108	21	3.30	100	4.00	280	4.00	-	109	121
EW14	-25	14.0	113	41	72	2.45	55	3.45	135	3.45	0.50	80	97
EW13	-10	28.0	225	162	63	2.75	115	4.20	410	4.20	0.80	90	115
EW11	-10	39.0	314	229	85	3.30	100	4.30	520	4.20	0.95	109	125
EW15	25	43.0	346	166	280	2.95	85	4.15	375	4.10	1.35	97	118
EW6	25	46.0	370	216	154	3.25	120	4.10	525	3.85	1.25	108	122
EW10	75	64.0	515	216	300	3.2	130	4.15	525	3.95	3.55	105	121
EW1	75	67.0	540	214	326	3.15	120	4.05	520	-	-	105	119
EW2	100	63.0	507	215	293	3.30	250	4.15	560	-	-	109	123
EW9	100	73.0	588	212	376	2.85	100	4.10	520	-	-	94	115
EW12	150	64.0	515	207	308	2.30	75	3.90	520	-	-	75	102
EW5	150	72.0	580	251	329	2.15	100	4.10	625	-	-	72	103
EW7	175	69.0	556	203	352	2.75	100	3.85	525	-	-	91	109
EW3	215	76.0	612	188	424	1.90	85	3.90	505	-	-	63	96
EW8	215	78.0	628	204	424	2.90	130	3.90	535	-	-	96	113
							HAZ Metal						
EH14	-150	23.0	185	117	68	3.90	90	4.70	255	4.60	0.15	129	143
EH3	-150	56.0	451	341	110	3.85	130	[illegible]	695	4.85	0.15	128	146
EH13	-100	26.0	209	185	24	3.60	110	[illegible]	400	4.75	-	118	138
EH7	- 50	32.0	258	205	52	3.25	130	[illegible]	475	4.75	0.20	108	133
EH1	- 50	85.0	684	337	347	3.85	120	4.90	680	4.35	-	127	145
EH8	0	78.0	628	362	266	3.35	85	4.95	705	4.50	0.15	111	137
EH2	0	144.0	1160	323	837	3.70	110	4.75	670	2.40	1.10	122	139
EH4	50	72.0	580	313	267	3.25	170	4.65	705	4.05	1.85	108	130
EH10	50	72.0	580	317	263	3.60	85	4.80	625	4.25	1.80	119	139
EH11	100	102.0	821	291	531	3.20	110	4.50	640	3.15	2.00	106	128
EH5	100	116.0	934	355	579	3.15	110	4.55	775	3.35	2.10	105	128
EH6	175	94.0	757	371	386	2.95	100	4.30	845	-	-	97	120
EH9	200	113.0	910	333	577	3.20	160	4.35	800	-	-	106	125
EH15	250	118.0	950	348	602	2.75	65	4.35	795	-		91	117
EH12	250	126.0	1015	334	680	2.55	70	4.20	775	-	-	85	112

TABLE 5-5

EFFECT OF IRRADIATION TO 3.79×10^{18} n/cm^2 (E > 1.0 MeV) AT 550°F

ON NOTCH TOUGHNESS PROPERTIES OF BRAIDWOOD UNIT 1 REACTOR VESSEL SURVEILLANCE MATERIALS

Material	Average 30 ft-lb Temperature (°F)			Average 35 mil Lateral Expansion Temperature (°F)			Average 50 ft-lb Temperature (°F)			Average Upper Shelf Energy at Full Shear (ft-lb)		
	Unirradiated	Irradiated	ΔT	Unirradiated	Irradiated	ΔT	Unirradiated	Irradiated	ΔT	Unirradiated	Irradiated	Δ(ft-lb)
Forging 490867-1/490813-1 (Tangential)	-65	-60	5	-45	-45	0	-40	-30	10	168	168	0
Forging 490867-1/490813-1 (Axial)	-45	-45	0	-15	-15	0	-15	-15	0	152	138	-14
Weld Metal	-20	-10	10	0	15	15	25	35	10	70	70	0
HAZ Metal	-170	-150	20	-180	-170	10	-140	-105	35	109	112	0

TABLE 5-6

COMPARISON OF BRAIDWOOD UNIT 1 SURVEILLANCE MATERIAL 30 FT-LB TRANSITION TEMPERATURE SHIFTS AND UPPER SHELF ENERGY DECREASES WITH REGULATORY GUIDE 1.99 REVISION 2 PREDICTIONS

		30 ft-lb Transition Temp. Shift		Upper Shelf Energy Decrease	
Material	Fluence 10^{18} n/cm^2	R.G. 1.99 Rev. 2 (Predicted) (°F)	Capsule U (°F)	R.G. 1.99 Rev. 2 (Predicted) (%)	Capsule U (%)
Forging 49D867-1/49D813-1 (Tang.)	3.79	15.0	5	15	0
Forging 49D867-1/49D813-1 (Axial)	3.79	15.0	0	15	9
Weld Metal	3.79	40.0	10	15	0

a) Cu and Ni values from Table 4-1 were used to determine R.G. 1.99 predictions.

TABLE 5-7

TENSILE PROPERTIES FOR BRAIDWOOD UNIT 1 REACTOR VESSEL SURVEILLANCE MATERIAL

IRRADIATED AT 550°F TO 3.79 x 10^{18} n/cm^2 (E > 1.0 MeV)

Material	Sample Number	Test Temp. (°F)	0.2% Yield Strength (ksi)	Ultimate Strength (ksi)	Fracture Load (kip)	Fracture Stress (ksi)	Fracture Strength (ksi)	Uniform Elongation (%)	Total Elongation (%)	Reduction in Area (%)
Forging 49D867-1/ 49C813-1 (Tangent. Orient.)	EL1	70	67.7	88.6	2.50	188.3	50.0	13.5	28.2	73
	EL2	300	61.1	79.5	2.30	149.4	46.9	10.5	24.6	69
	EL3	550	58.6	83.5	2.50	147.9	50.0	11.2	23.8	66
Forging 49D867-1/ 49C813-1 (Axial Orient.)	ET1	70	69.8	89.6	2.80	181.9	57.0	11.3	24.2	61
	ET2	300	62.8	81.0	2.60	181.6	53.0	9.0	21.9	61
	ET3	550	58.6	84.5	2.80	153.3	57.0	9.8	20.4	63
Weld	EW1	70	73.8	90.7	3.25	117.7	66.2	10.5	21.2	61
Weld	EW2	300	70.8	85.8	2.95	151.4	60.1	8.3	18.9	60
Weld	EW3	550	68.8	85.6	3.20	181.1	65.2	8.3	17.4	56

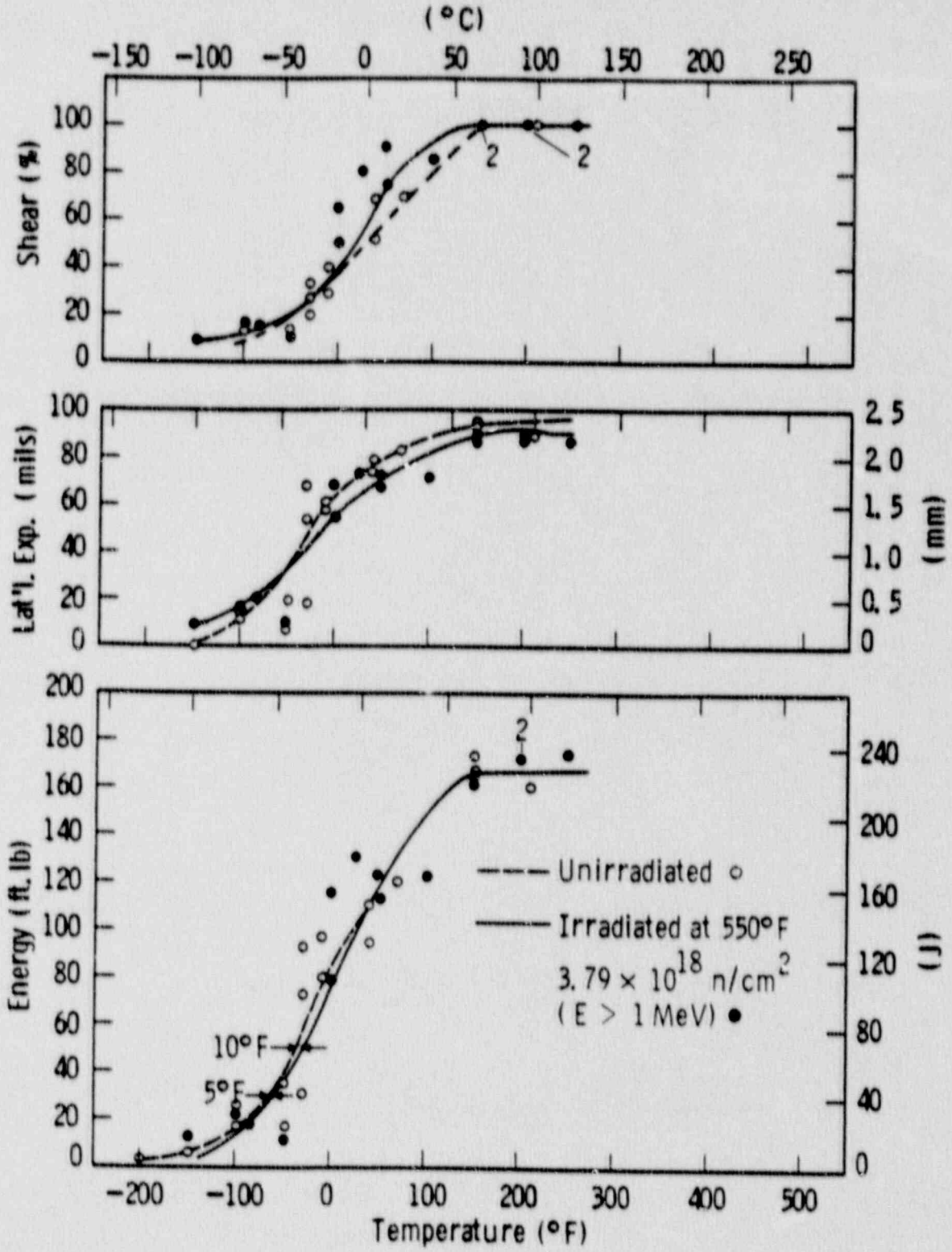

Figure 5-1. Charpy V-Notch Impact Properties for Braidwood Unit 1 Reactor Vessel Shell Forging 49D867-1/49C813-1 (Tangential Orientation)

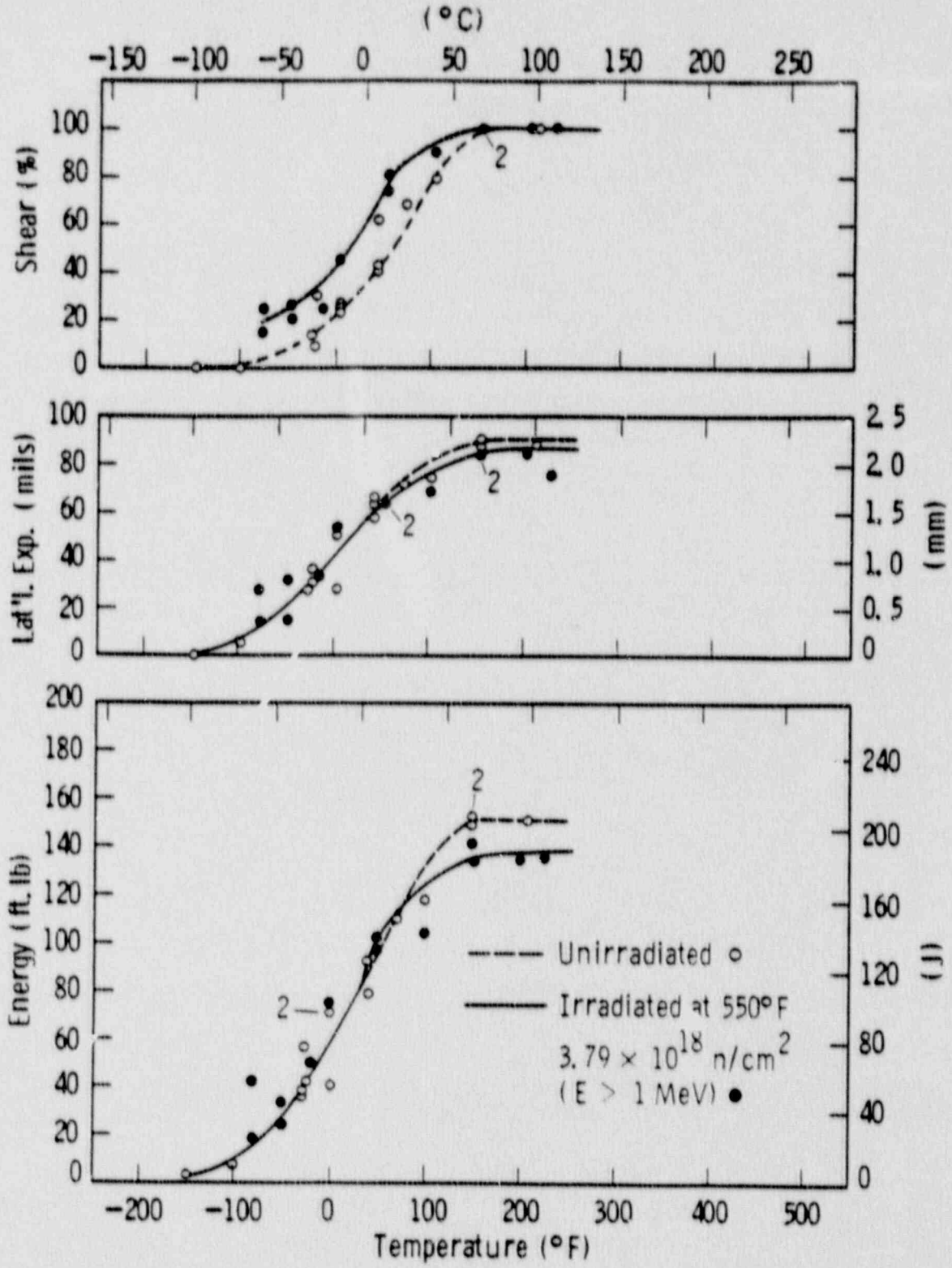

Figure 5-2. Charpy V-Notch Impact Properties for Braidwood Unit 1 Reactor Vessel Shell Forging 49D867-1/49C813-1 (Axial Orientation)

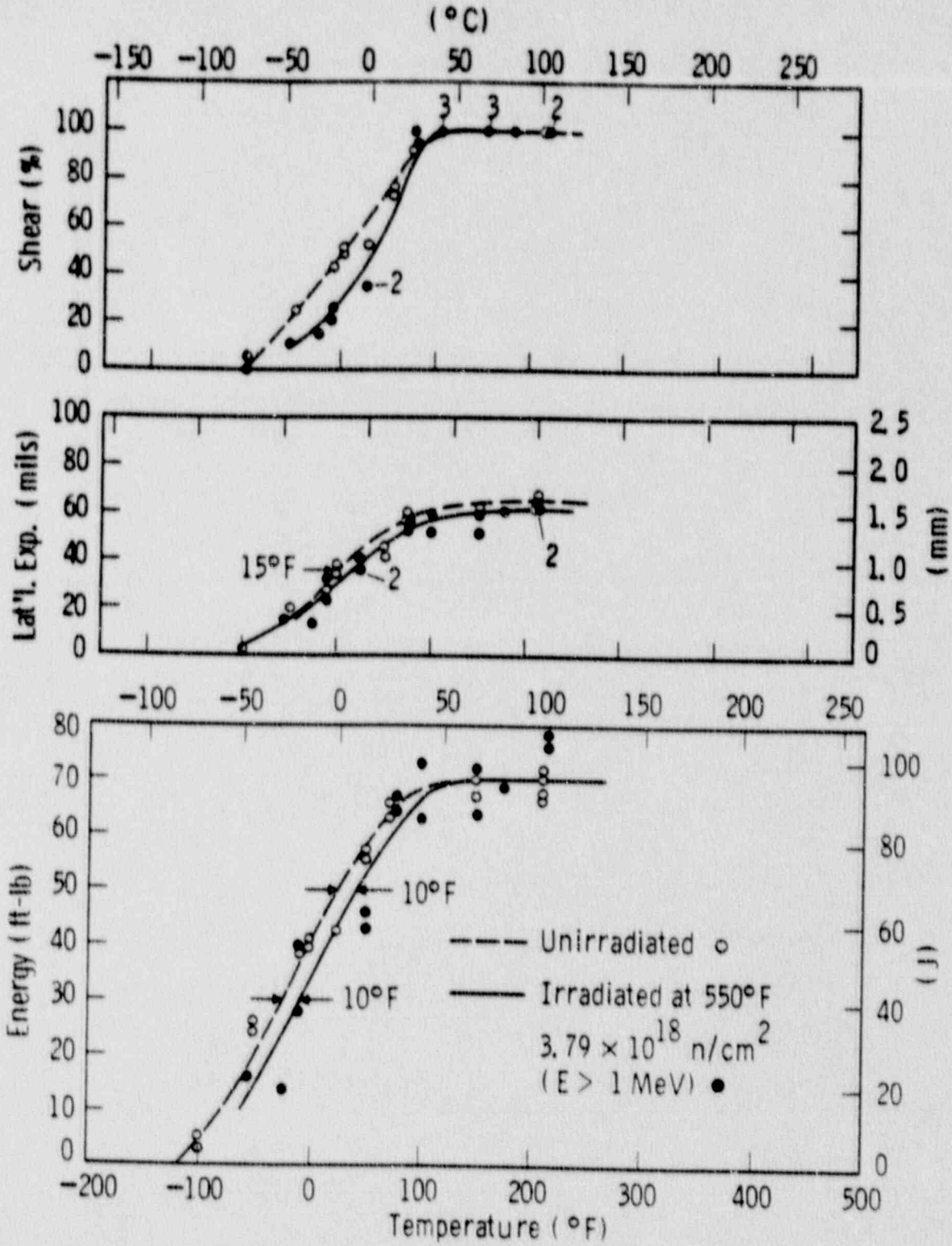

Figure 5-3. Charpy V-Notch Impact Properties for Braidwood Unit 1 Reactor Vessel Weld Metal

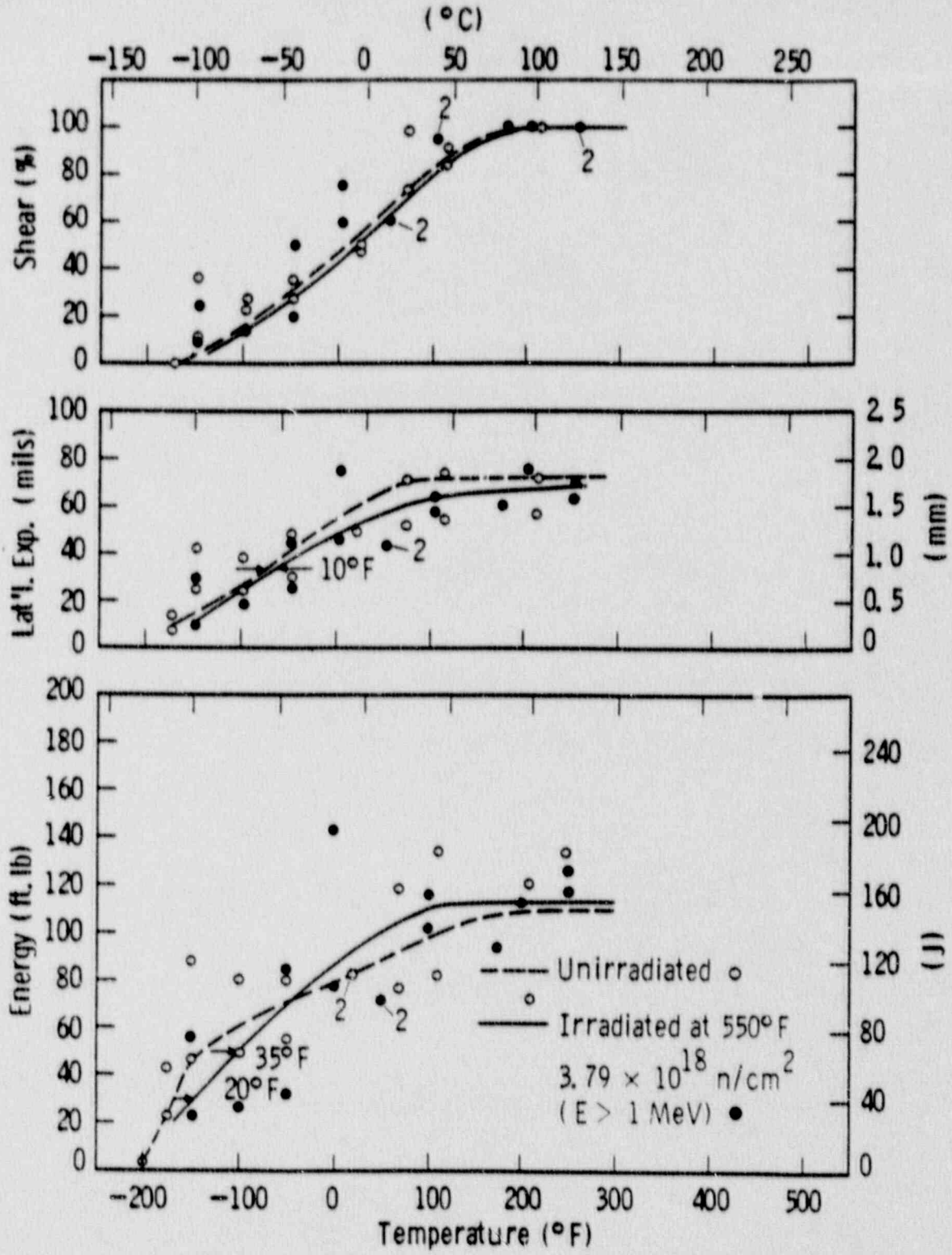

Figure 5-4. Charpy V-Notch Impact Properties for Braidwood Unit 1 Reactor Weld Heat Affected Zone Metal

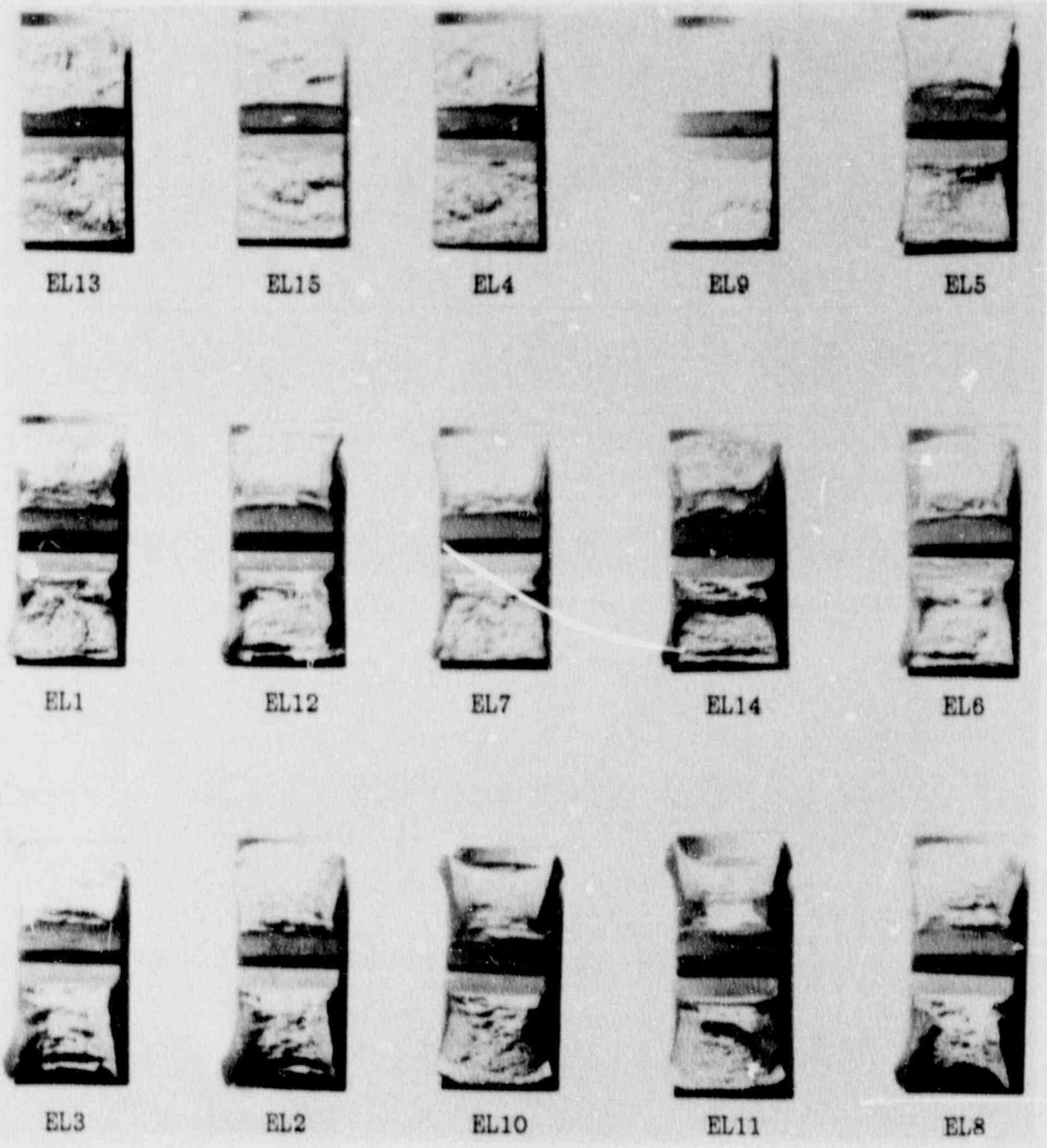

Figure 5-5. Charpy Impact Specimen Fracture Surfaces for Braidwood Unit 1 Reactor Vessel Shell Forging 48D867-1/49C813-1 (Tangential Orientation)

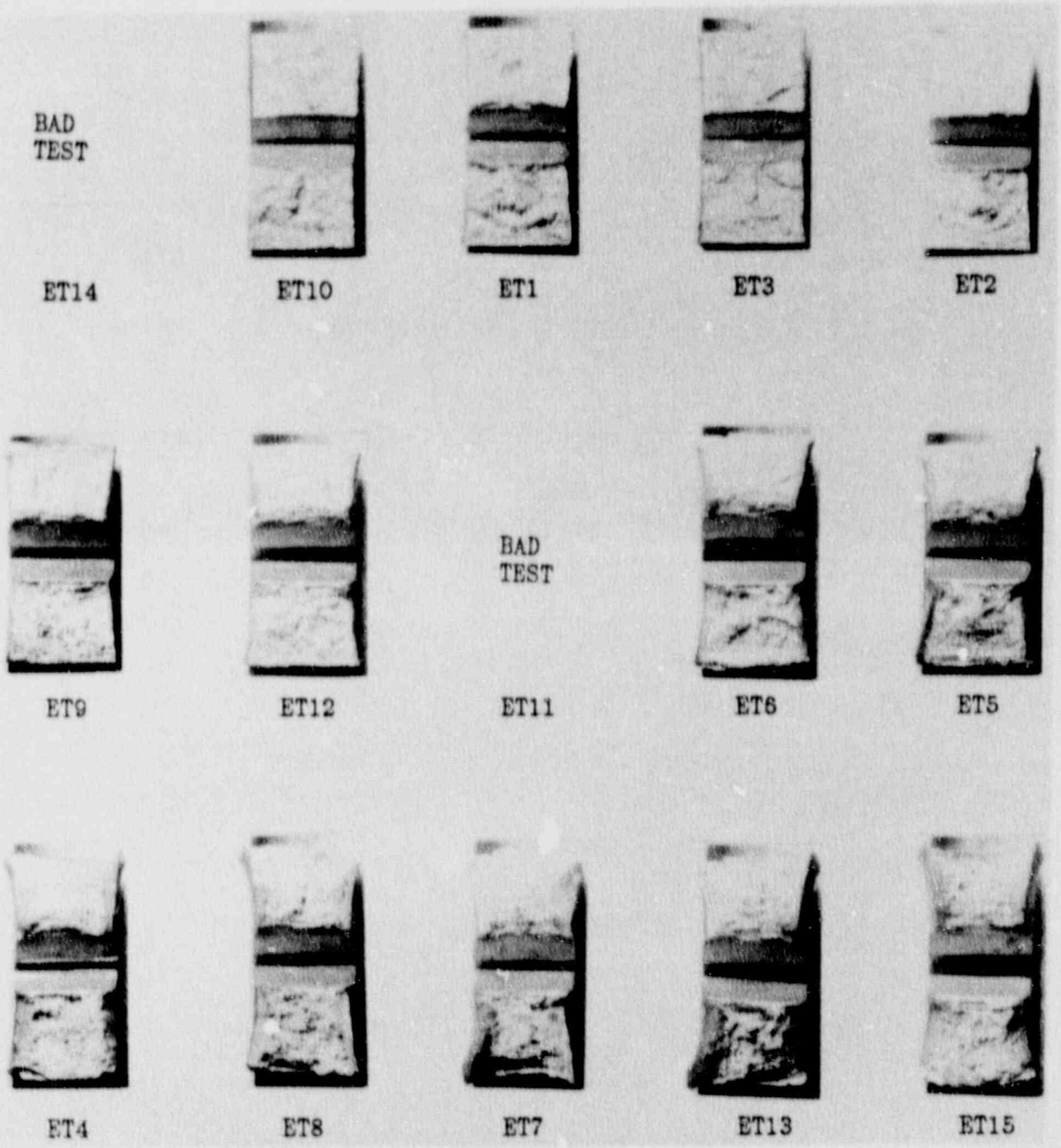

Figure 5-6. Charpy Impact Specimen Fracture Surfaces for Braidwood Unit 1 Reactor Vessel Shell Forging 49D867-1/49C813-1 (Axial Orientation)

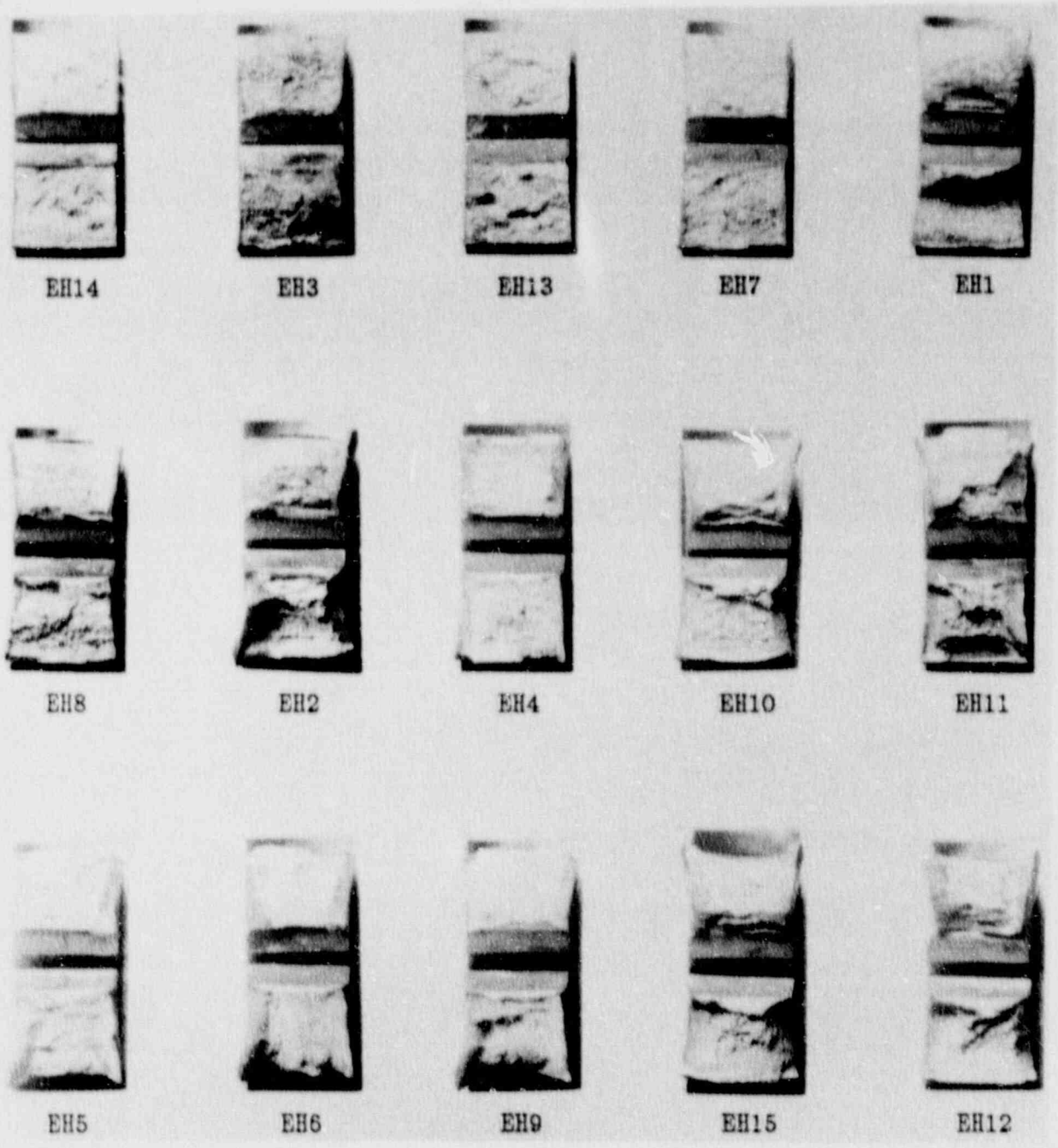

Figure 5-7. Charpy Impact Specimen Fracture Surfaces for Braidwood Unit 1 Reactor Vessel Weld Metal

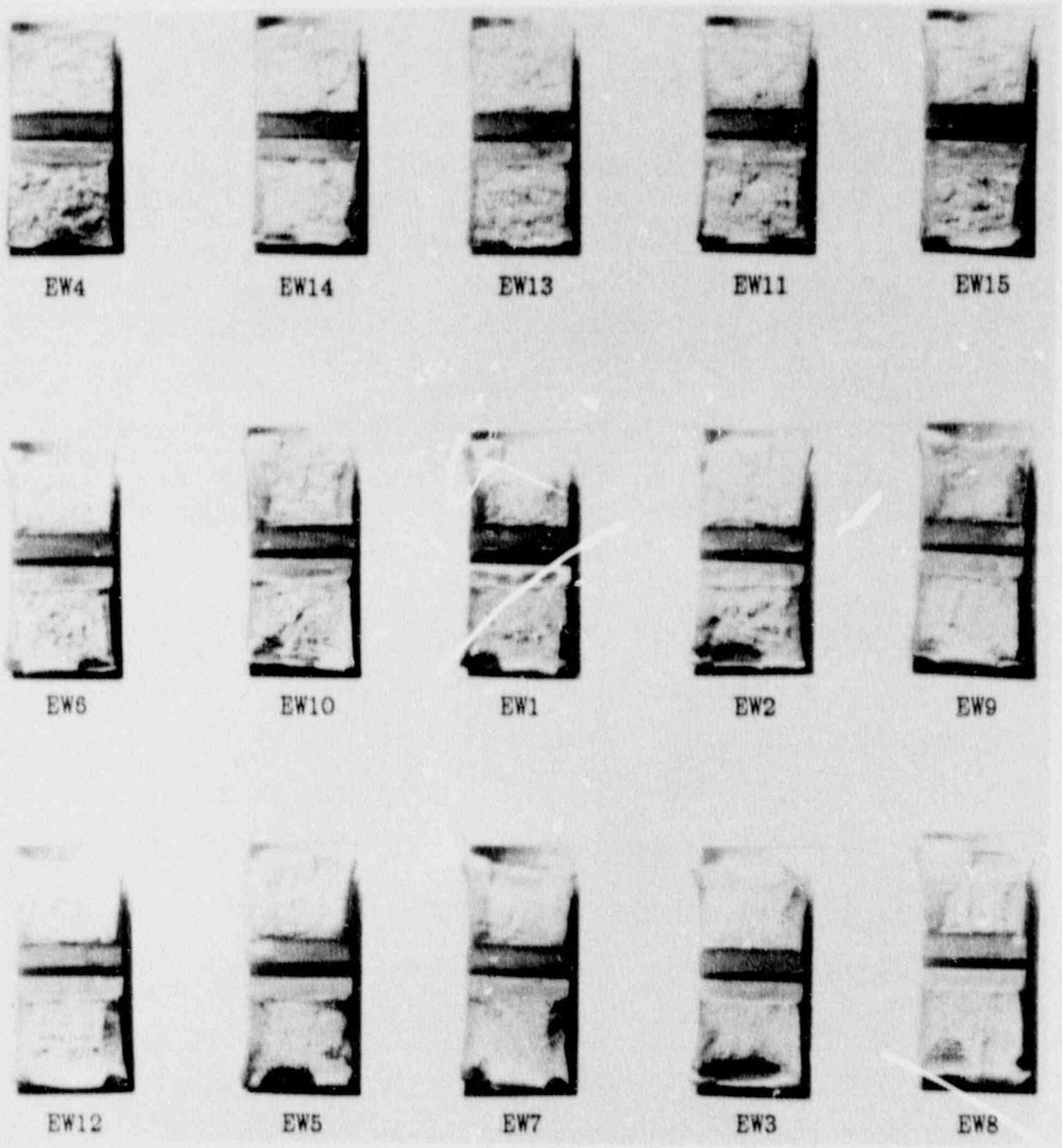

Figure 5-8. Charpy Impact Specimen Fracture Surfaces for Braidwood Unit 1 Reactor Vessel Weld Heat Affected Zone (HAZ) Metal

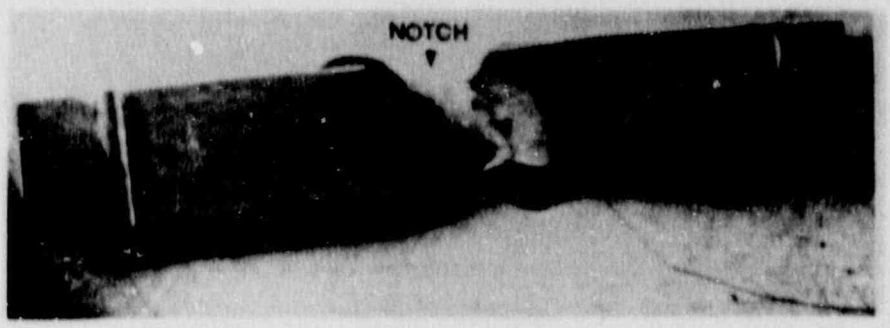

(a) ET11

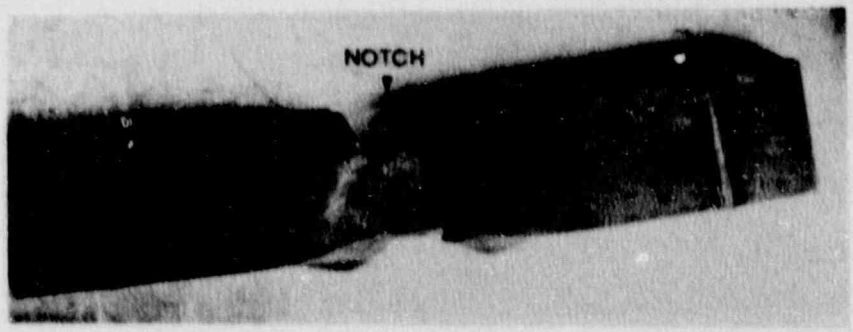

(b) ET14

Figure 5-9. Photographs of Capsule U Specimens (a) ET11 and (b) ET14

(a) EH 2

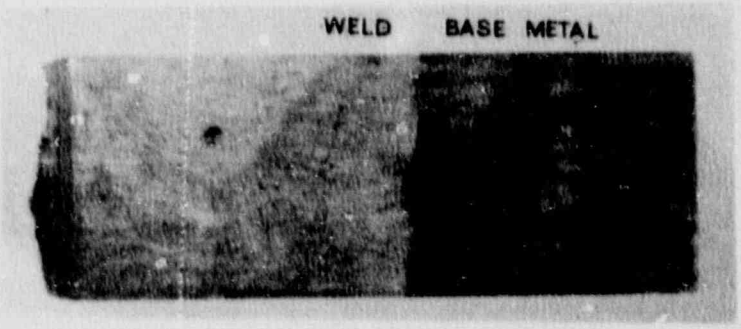

(b) EW14

Figure 5-10. (a) Photograph of Capsule U Specimen EH2, and (b) Photograph of Capsule U Specimen EW14

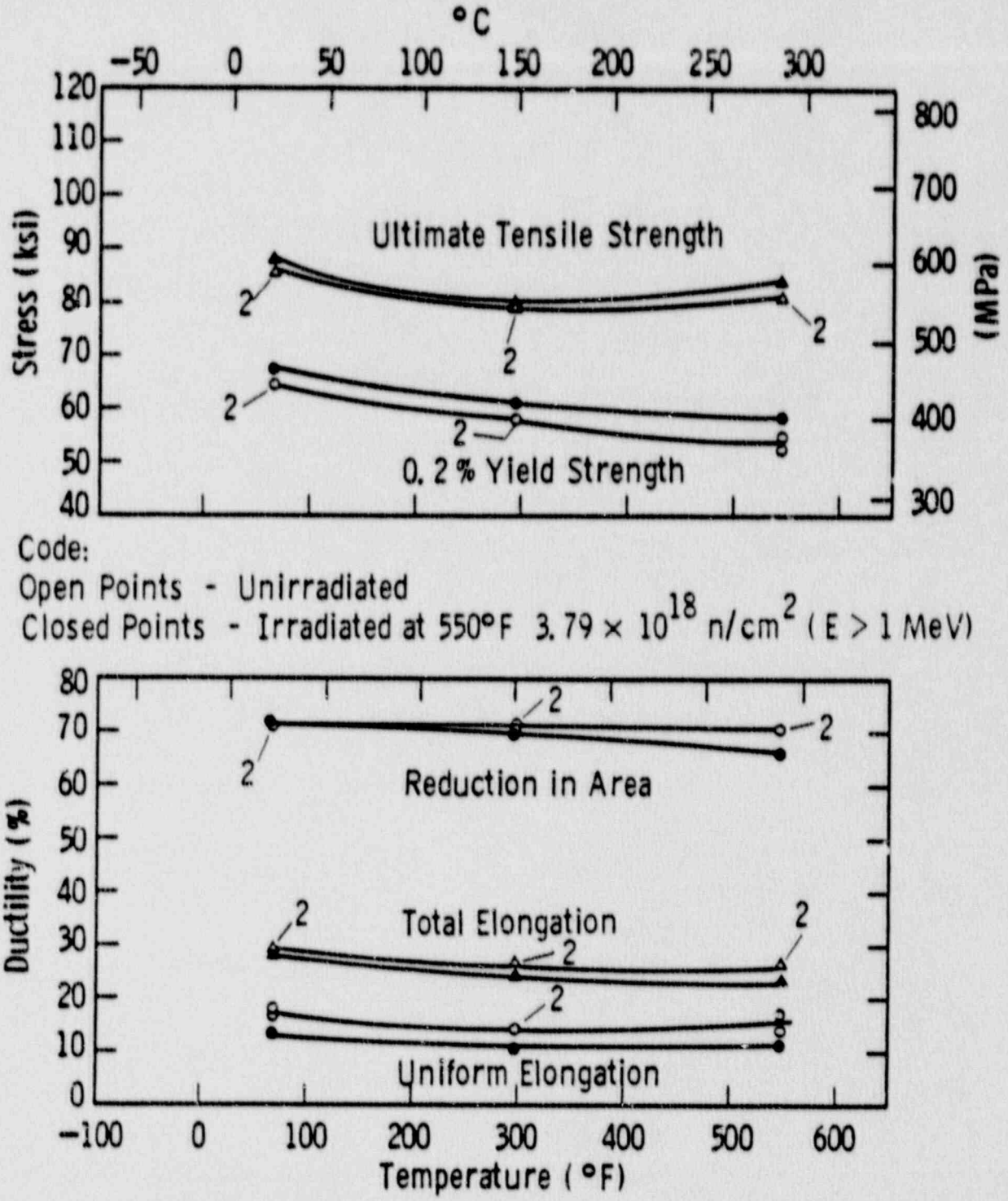

Figure 5-11. Tensile Properties for Braidwood Unit 1 Reactor Vessel Shell Forging 49D867-1/49C813-1 (Tangential Orientation)

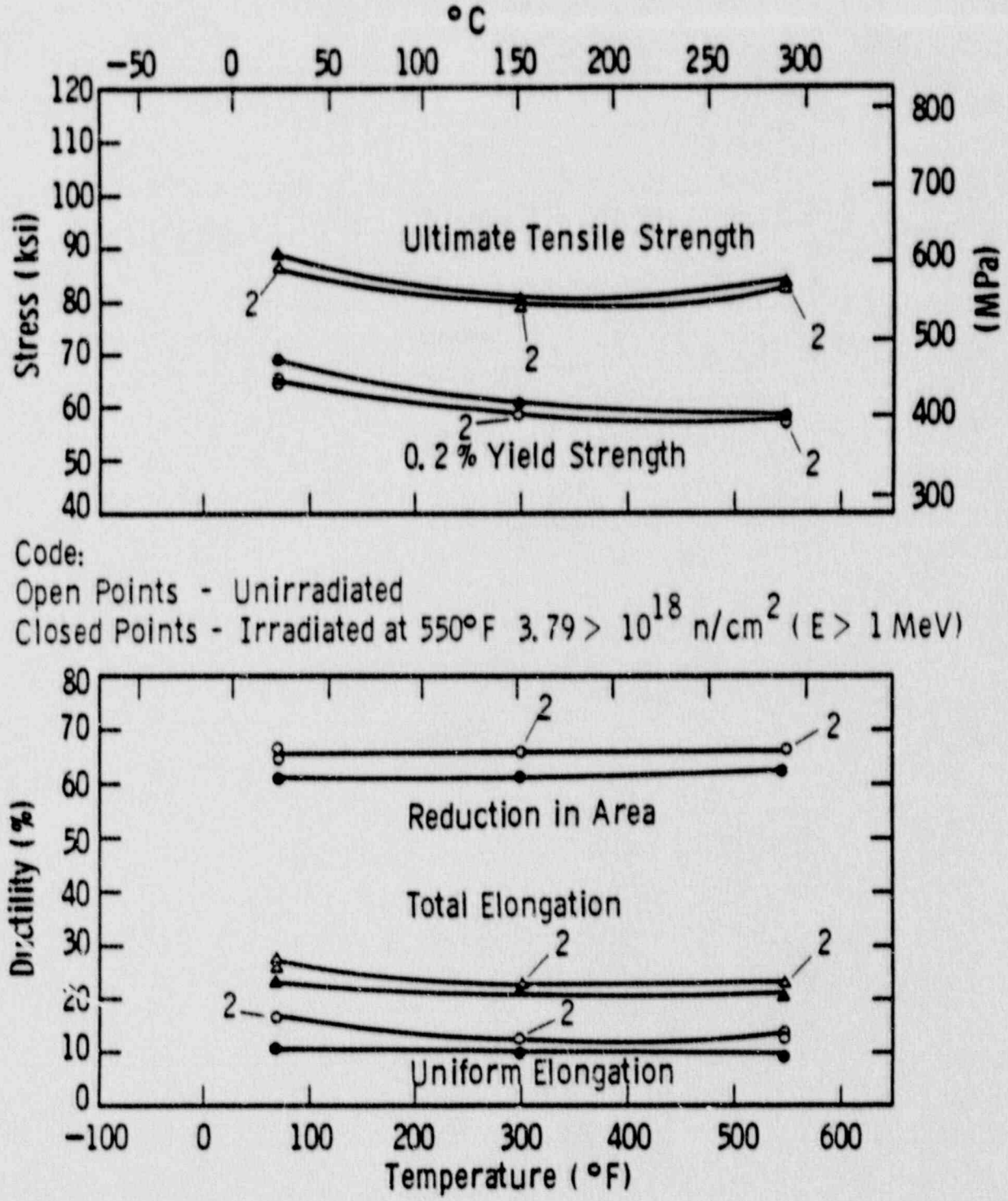

Figure 5-12. Tensile Properties for Braidwood Unit 1 Reactor Vessel Shell Forging 49D867-1/49C813-1 (Axial Orientation)

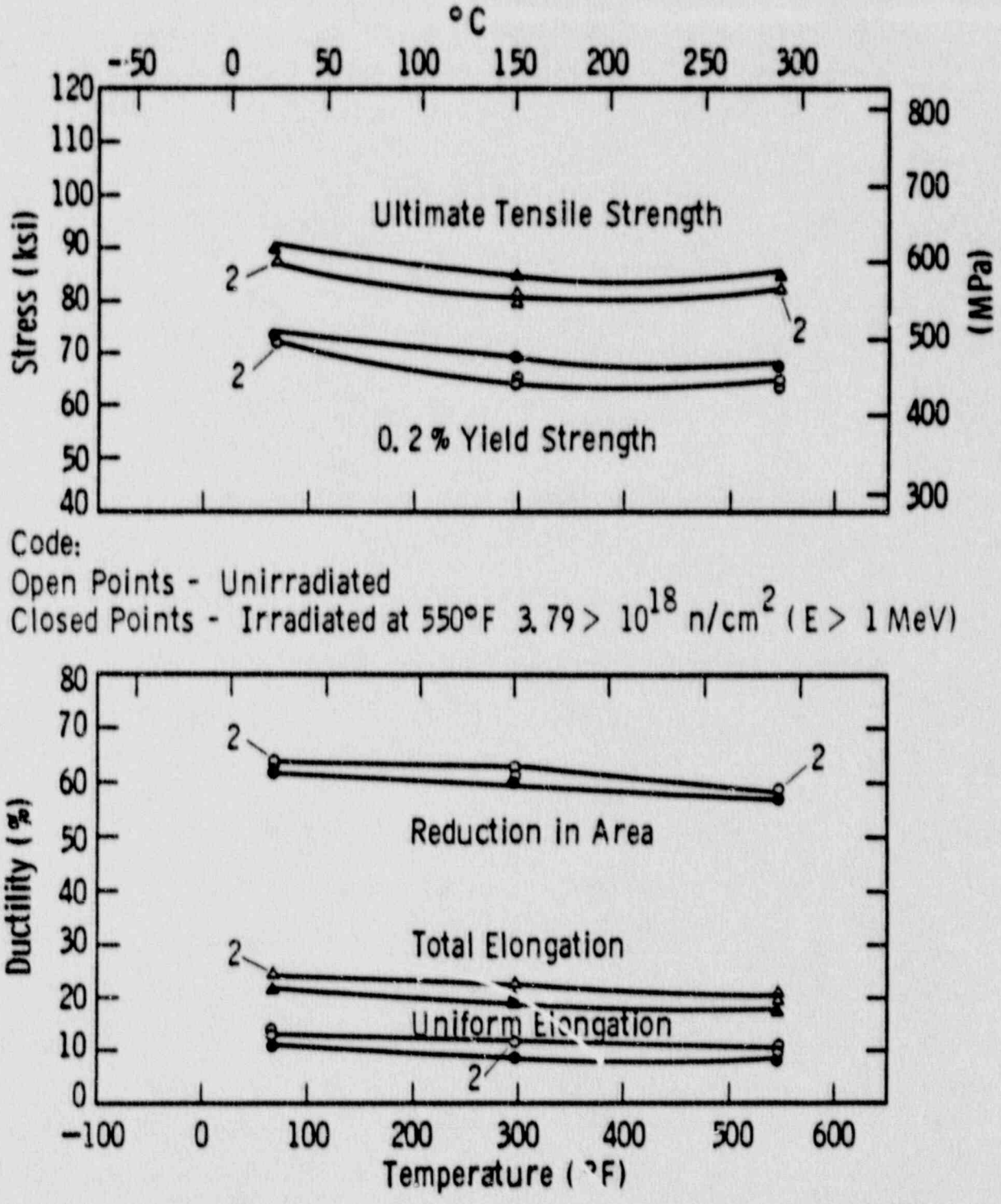

Figure 5-13. Tensile Properties for Braidwood Unit 1 Reactor Vessel Weld Metal

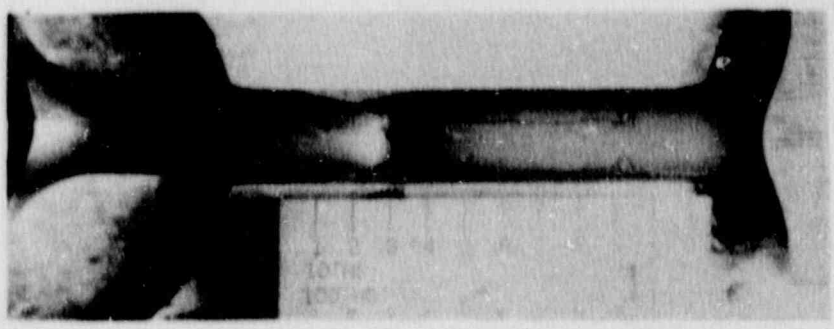

Specimen EL1 70°F

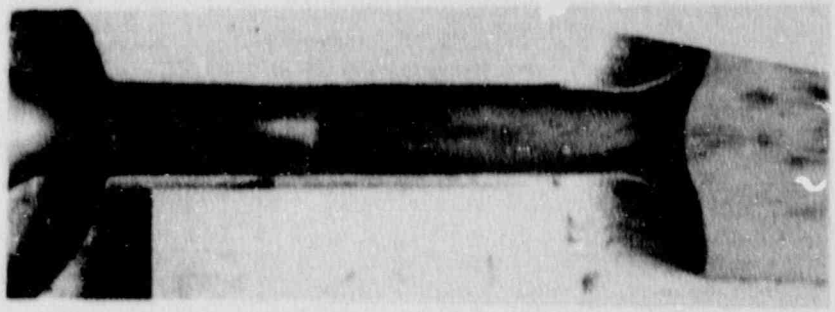

Specimen EL2 300°F

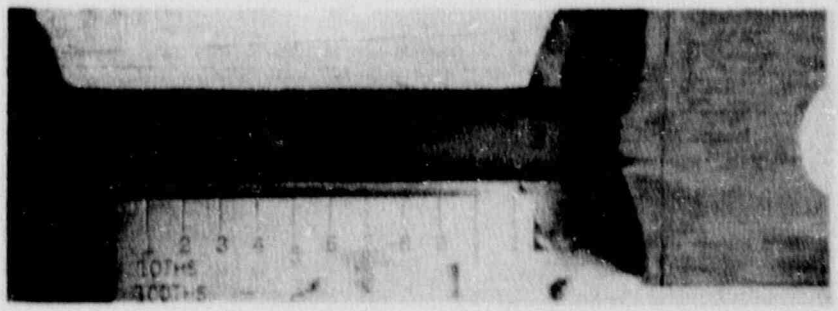

Specimen EL3 550°F

Figure 5-14. Fractured Tensile Specimens from Braidwood Unit 1 Reactor Vessel Shell Forging 49D867-1/49C813-1 (Tangential Orientation)

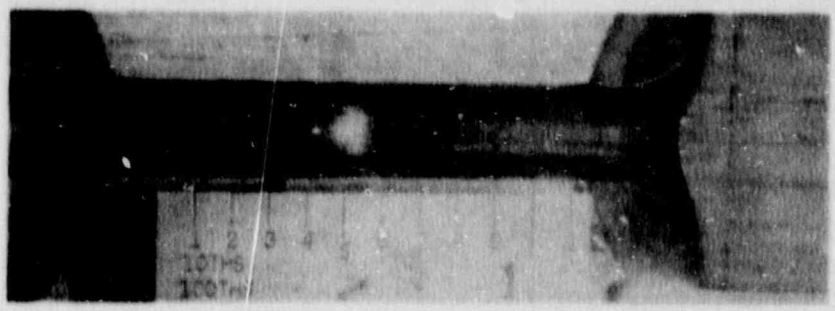

Specimen ET1 70°F

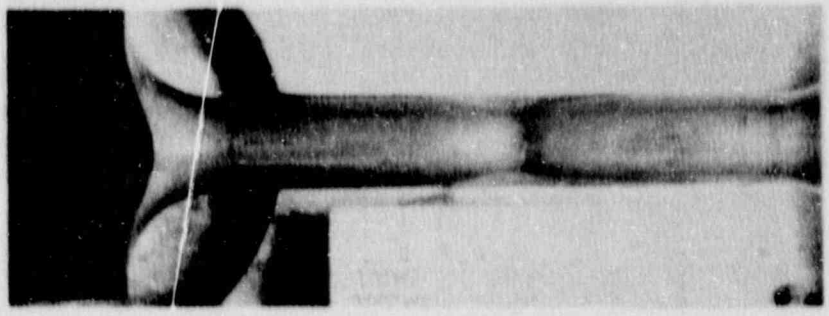

Specimen ET2 300°F

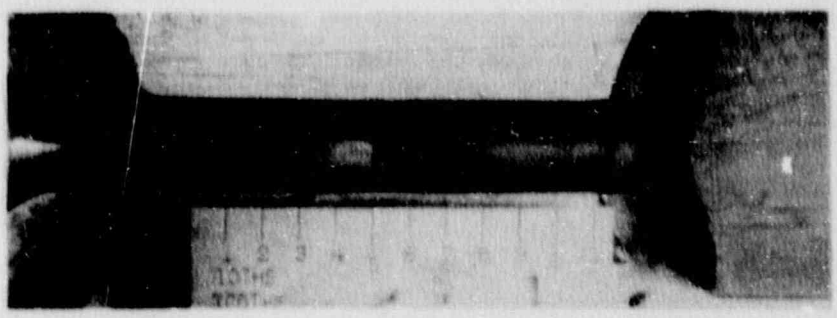

Specimen ET3 550°F

Figure 5-15. Fractured Tensile Specimens from Braidwood Unit 1 Reactor Vessel Shell Forging 49D867-1/49C813-1 (Axial Orientation)

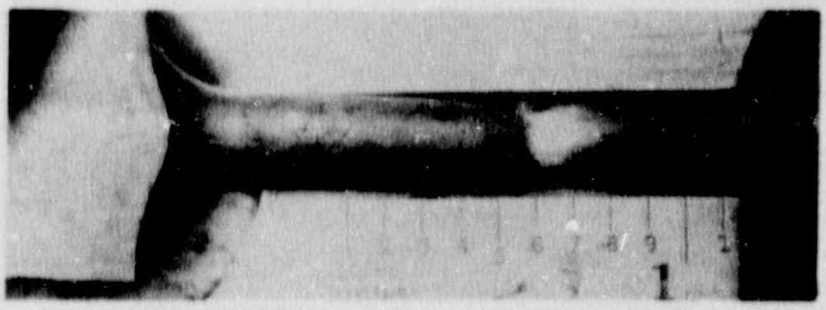

Specimen EW1 70°F

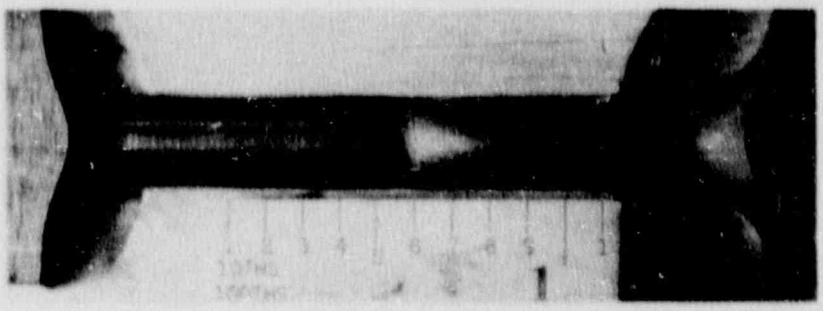

Specimen EW2 300°F

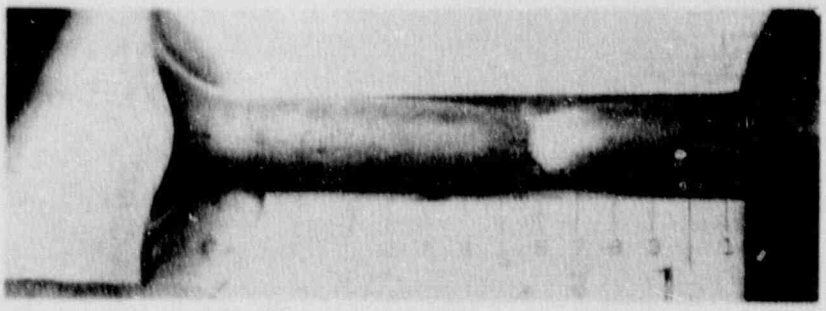

Specimen EW3 550°F

Figure 5-16. Fractured Tensile Specimens from Braidwood Unit 1 Reactor Vessel Weld Metal

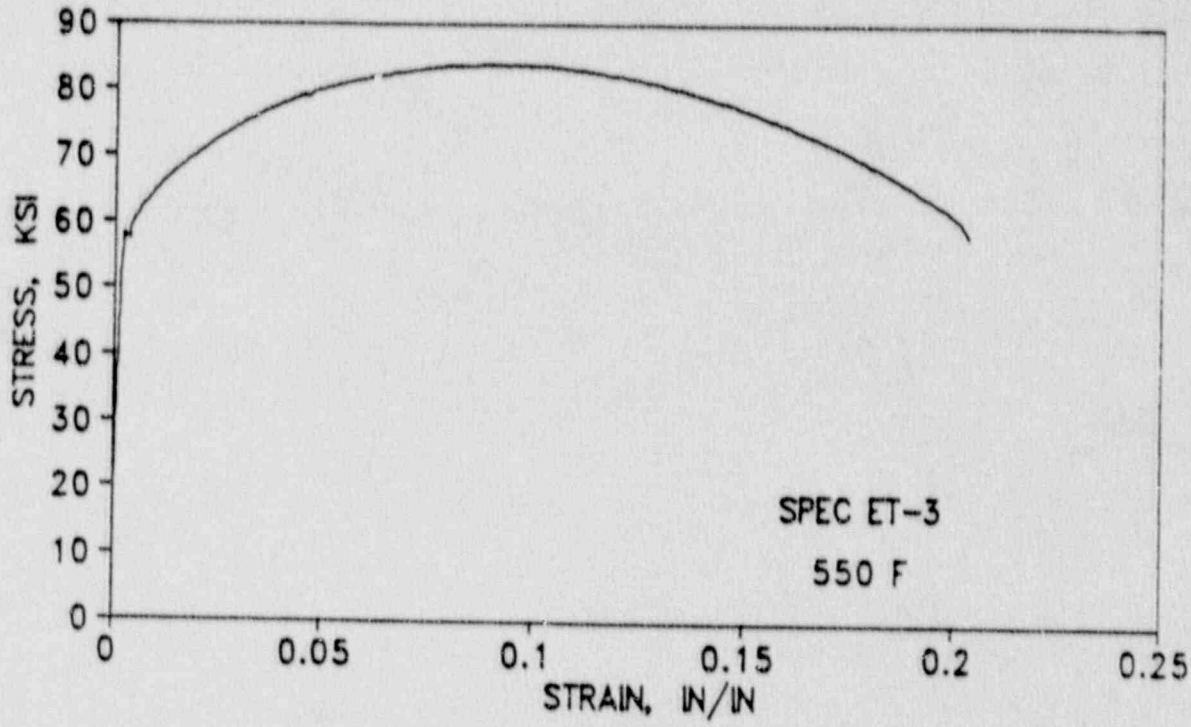

Figure 5-17. Typical Stress-Strain Curve for Braidwood Unit 1 Shell Forging 49D867-1/49C813-1 Tension Specimens.

SECTION 6.0
RADIATION ANALYSIS AND NEUTRON DOSIMETRY

6.1 Introduction

Knowledge of the neutron environment within the reactor pressure vessel and surveillance capsule geometry is required as an integral part of LWR reactor pressure vessel surveillance programs for two reasons. First, in order to interpret the neutron radiation-induced material property changes observed in the test specimens, the neutron environment (energy spectrum, flux, fluence) to which the test specimens were exposed must be known. Second, in order to relate the changes observed in the test specimens to the present and future condition of the reactor vessel, a relationship must be established between the neutron environment at various positions within the reactor vessel and that experienced by the test specimens. The former requirement is normally met by employing a combination of rigorous analytical techniques and measurements obtained with passive neutron flux monitors contained in each of the surveillance capsules. The latter information is derived solely from analysis.

The use of fast neutron fluence ($E > 1.0$ MeV) to correlate measured materials properties changes to the neutron exposure of the material for light water reactor applications has traditionally been accepted for development of damage trend curves as well as for the implementation of trend curve data to assess vessel condition. In recent years, however, it has been suggested that an exposure model that accounts for differences in neutron energy spectra between surveillance capsule locations and positions within the vessel wall could lead to an improvement in the uncertainties associated with damage trend curves as well as to a more accurate evaluation of damage gradients through the pressure vessel wall.

Because of this potential shift away from a threshold fluence toward an energy dependent damage function for data correlation, ASTM Standard Practice E853, "Analysis and Interpretation of Light Water Reactor Surveillance Results," recommends reporting displacements per iron atom (dpa) along with fluence

(E > 1.0 MeV) to provide a data base for future reference. The energy dependent dpa function to be used for this evaluation is specified in ASTM Standard Practice E693, "Characterizing Neutron Exposures in Ferritic Steels in Terms of Displacements per Atom." The application of the dpa parameter to the assessment of embrittlement gradients through the thickness of the pressure vessel wall has already been promulgated in Revision 2 to the Regulatory Guide 1.99, "Radiation Damage to Reactor Vessel Materials."

This section provides the results of the neutron dosimetry evaluations performed in conjunction with the analysis of test specimens contained in surveillance capsule U. Fast neutron exposure parameters in terms of fast neutron fluence (E > 1.0 MeV), fast neutron fluence (E > 0.1 MeV), and iron atom displacements (dpa) are established for the capsule irradiation history. The analytical formalism relating the measured capsule exposure to the exposure of the vessel wall is described and used to project the integrated exposure of the vessel itself. Also uncertainties associated with the derived exposure parameters at the surveillance capsule and with the projected exposure of the pressure vessel are provided.

6.2 Discrete Ordinates Analysis

A plan view of the reactor geometry at the core midplane is shown in Figure 4-1. Six irradiation capsules attached to the neutron pads are included in the reactor design to constitute the reactor vessel surveillance program. The capsules are located at azimuthal angles of 58.5°, 61.0°, 121.5°, 238.5°, 241.0°, and 301.5° relative to the core cardinal axes as shown in Figure 4-1.

A plan view of a dual surveillance capsule holder attached to the neutron pad is shown in Figure 6-1. The stainless steel specimen containers are 1.182 by 1-inch and approximately 56 inches in height. The containers are positioned axially such that the specimens are centered on the core midplane, thus spanning the central 5 feet of the 12-foot high reactor core.

From a neutron transport standpoint, the surveillance capsule structures are significant. They have a marked effect on both the distribution of neutron flux and the neutron energy spectrum in the water annulus between the neutron pad and the reactor vessel. In order to properly determine the neutron environment at the test specimen locations, the capsules themselves must be included in the analytical model.

In performing the fast neutron exposure evaluations for the surveillance capsules and reactor vessel, two distinct sets of transport calculations were carried out. The first, a single computation in the conventional forward mode, was used primarily to obtain relative neutron energy distributions throughout the reactor geometry as well as to establish relative radial distributions of exposure parameters {ϕ(E > 1.0 Mev), ϕ(E > 0.1 Mev), and dpa} through the vessel wall. The neutron spectral information was required for the interpretation of neutron dosimetry withdrawn from the surveillance capsule as well as for the determination of exposure parameter ratios; i.e., dpa/ϕ(E > 1.0 MeV), within the pressure vessel geometry. The relative radial gradient information was required to permit the projection of measured exposure parameters to locations interior to the pressure vessel wall; i.e., the 1/4T, 1/2T, and 3/4T locations.

The second set of calculations consisted of a series of adjoint analyses relating the fast neutron flux (E > 1.0 MeV) at surveillance capsule positions, and several azimuthal locations on the pressure vessel inner radius to neutron source distributions within the reactor core. The importance functions generated from these adjoint analyses provided the basis for all absolute exposure projections and comparison with measurement. These importance functions, when combined with cycle specific neutron source distributions, yielded absolute predictions of neutron exposure at the locations of interest for the cycle 1 irradiation; and established the means to perform similar predictions and dosimetry evaluations for all subsequent fuel cycles. It is important to note that the cycle specific neutron source distributions utilized in these analyses included not only spatial variations of fission rates within the reactor core; but, also accounted for the effects

of varying neutron yield per fission and fission spectrum introduced by the build-up of plutonium as the burnup of individual fuel assemblies increased.

The absolute cycle specific data from the adjoint evaluations together with relative neutron energy spectra and radial distribution information from the forward calculation provided the means to:

1. Evaluate neutron dosimetry obtained from surveillance capsule locations.

2. Extrapolate dosimetry results to key locations at the inner radius and through the thickness of the pressure vessel wall.

3. Enable a direct comparison of analytical prediction with measurement.

4. Establish a mechanism for projection of pressure vessel exposure as the design of each new fuel cycle evolves.

The forward transport calculation for the reactor model summarized in Figures 4-1 and 6-1 was carried out in R, Θ geometry using the DOT two-dimensional discrete ordinates code [12] and the SAILOR cross-section library [13]. The SAILOR library is a 47 group ENDFB-IV based data set produced specifically for light water reactor applications. In these analyses anisotopic scattering was treated with a P_3 expansion of the cross-sections and the angular discretization was modeled with an S_8 order of angular quadrature.

The reference core power distribution utilized in the forward analysis was derived from statistical studies of long-term operation of Westinghouse 4-loop plants. Inherent in the development of this reference core power distribution is the use of an out-in fuel management strategy; i.e., fresh fuel on the core periphery. Furthermore, for the peripheral fuel assemblies, a 2σ uncertainty derived from the statistical evaluation of plant to plant and cycle to cycle variations in peripheral power was used. Since it is unlikely that a single reactor would have a power distribution at the nominal $+2\sigma$

level for a large number of fuel cycles, the use of this reference distribution is expected to yield somewhat conservative results.

All adjoint analyses were also carried out using an S_8 order of angular quadrature and the P_3 cross-section approximation from the SAILOR library. Adjoint source locations were chosen at several azimuthal locations along the pressure vessel inner radius as well as the geometric center of each surveillance capsule. Again, these calculations were run in R, Θ geometry to provide neutron source distribution importance functions for the exposure parameter of interest; in this case, ϕ (E > 1.0 MeV). Having the importance functions and appropriate core source distributions, the response of interest could be calculated as:

$$R(r, \Theta) = \int_r \int_\Theta \int_E I(r, \Theta, E)\, S(r, \Theta, E)\, r\, dr\, d\Theta\, dE$$

where: $R(r, \Theta)$ = ϕ (E > 1.0 MeV) at radius r and azimuthal angle Θ

$I(r, \Theta, E)$ = Adjoint importance function at radius, r, azimuthal angle Θ, and neutron source energy E.

$S(r, \Theta, E)$ = Neutron source strength at core location r, Θ and energy E.

Although the adjoint importance functions used in the Braidwood Unit 1 analysis were based on a response function defined by the threshold neutron flux (E > 1.0 MeV), prior calculations have shown that, while the implementation of low leakage loading patterns significantly impact the magnitude and the spatial distribution of the neutron field, changes in the relative neutron energy spectrum are of second order. Thus, for a given location the ratio of dpa/ϕ (E > 1.0 MeV) is insensitive to changing core source distributions. In the application of these adjoint important functions to the Braidwood Unit 1 reactor, therefore, the iron displacement rates (dpa) and the neutron flux (E > 0.1 MeV) were computed on a cycle specific basis by using dpa/ϕ (E > 1.0 MeV) and ϕ (E > 0.1 MeV)/ϕ (E > 1.0 MeV) ratios from the forward analysis in conjunction with the cycle specific ϕ (E > 1.0 MeV) solutions from the individual adjoint evaluations.

The reactor core power distribution used in the plant specific adjoint calculations was taken from the fuel cycle design report for the first operating cycle of Braidwood Unit 1 [14]. The relative power levels in fuel assemblies that are significant contributors to the neutron exposure of the pressure vessel and surveillance capsules are summarized in Figure 6-2. For comparison purposes, the core power distribution (design basis) used in the reference forward calculation is also illustrated in Figure 6-2.

Selected results from the neutron transport analyses performed for the Braidwood Unit 1 reactor are provided in Tables 6-1 through 6-5. The data listed in these tables establish the means for absolute comparisons of analysis and measurement for the capsule irradiation period and provide the means to correlate dosimetry results with the corresponding neutron exposure of the pressure vessel wall.

In Table 6-1, the calculated exposure parameters [ϕ (E > 1.0 MeV), ϕ (E > 0.1 MeV), and dpa] are given at the geometric center of the two surveillance capsule positions for both the design basis and the plant specific core power distributions. The plant specific data, based on the adjoint transport analysis, are meant to establish the absolute comparison of measurement with analysis. The design basis data derived from the forward calculation are provided as a point of reference against which plant specific fluence evaluations can be compared. Similar data is given in Table 6-2 for the pressure vessel inner radius. Again, the three pertinent exposure parameters are listed for both the design basis and the cycle 1 plant specific power distributions. It is important to note that the data for the vessel inner radius were taken at the clad/base metal interface and, thus, represent the maximum exposure levels of the vessel wall itself.

Radial gradient information for neutron flux (E > 1.0 MeV), neutron flux (E > 0.1 MeV), and iron atom displacement rate is given in Tables 6-3, 6-4, and 6-5, respectively. The data, obtained from the forward neutron transport calculation, are presented on a relative basis for each exposure parameter at several azimuthal locations. Exposure parameter distributions within the wall may be obtained by normalizing the calculated or projected exposure at the vessel inner radius to the gradient data given in Tables 6-3 through 6-5.

Values of key fast neutron exposure parameters were derived from the measured reaction rates using the FERRET least square adjustment code [29]. The FERRET approach used the measured reaction rate data and the calculated neutron energy spectrum at the the center of the surveillance capsule as input and proceeded to adjust a priori (calculated) group fluxes to produce a best fit (in a least squares sense) to the reaction rate data. The exposure parameters along with associated uncertainties where then obtained from the adjusted spectra.

In the FERRET evaluations, a log normal least-squares algorithm weights both the a priori values and the measured data in accordance with the assigned uncertainties and correlations. In general, the measured values f are linearly related to the flux ϕ by some response matrix A:

$$f_i^{(s,\alpha)} = \sum_g A_{ig}^{(s)} \phi_g^{(\alpha)}$$

where i indexes the measured values belonging to a single data set s, g designates the energy group and α delineates spectra that may be simultaneously adjusted. For example,

$$R_i = \sum_g \sigma_{ig} \phi_g$$

relates a set of measured reaction rates R_i to a single spectrum ϕ_g by the multigroup cross section σ_{ig}. (In this case, FERRET also adjusts the cross-sections.) The lognormal approach automatically accounts for the physical constraint of positive fluxes, even with the large assigned uncertainties.

In the FERRET analysis of the dosimetry data, the continuous quantities (i.e., fluxes and cross-sections) were approximated in 53 groups. The calculated fluxes from the discrete ordinates analysis were expanded into the FERRET group structure using the SAND-II code [30]. This procedure was carried out by first expanding the a priori spectrum into the SAND-II 620 group structure using a SPLINE interpolation procedure for interpolation in regions where group boundaries do not coincide. The 620-point spectrum was then easily collapsed to the group scheme used in FERRET.

The cross-sections were also collapsed into the 53 energy-group structure using SAND II with calculated spectra (as expanded to 620 groups) as weighting functions. The cross sections were taken from the ENDF/B-V dosimetry file. Uncertainty estimates and 53 x 53 covariance matrices were constructed for each cross section. Correlations between cross sections were neglected due to data and code limitations, but are expected to be unimportant.

For each set of data or a priori values, the inverse of the corresponding relative covariance matrix M is used as a statistical weight. In some cases, as for the cross sections, a multigroup covariance matrix is used. More often, a simple parameterized form is used:

$$M_{gg'} = R_N^2 + R_g R_{g'} P_{gg'}$$

where R_N specifies an overall fractional normalization uncertainty (i.e., complete correlation) for the corresponding set of values. The fractional uncertainties R_g specify additional random uncertainties for group g that are correlated with a correlation matrix:

$$P_{gg'} = (1 - \Theta)\, \delta_{gg'} + \Theta \exp\left[\frac{-(g-g')^2}{2\theta^2}\right]$$

For example, the neutron flux (E > 1.0 MeV) at the 1/4T position on the 45° azimuth is given by:

$$\phi_{1/4T}(45°) = \phi(220.27, 45°)\ F\ (225.75, 45°)$$

where $\phi_{1/4T}(45°)$ = Projected neutron flux at the 1/4T position on the 45° azimuth

$\phi\ (220.27, 45°)$ = Projected or calculated neutron flux at the vessel inner radius on the 45° azimuth.

$F\ (225.75, 45°)$ = Relative radial distribution function from Table 6-3.

Similar expressions apply for exposure parameters in terms of ϕ(E > 0.1 MeV) and dpa/sec.

The DOT calculations were carried out for a typical octant of the reactor. However, for the neutron pad arrangement in Braidwood Unit 1, the pad extent for all octants is not the same. For the analysis of the flux to the pressure vessel, an octant was chosen with the neutron pad extending from 32.5° to 45° (12.5°) which produces the maximum vessel flux. Other octants have neutron pads extending 22.5° or 20° which provide more shielding. For the octant with the 12.5° pad, the maximum flux to the vessel occurs near 25° and the values in the tables for the 25° angle are vessel maximum values. Exposure values for 0°, 15°, and 45° can be used for all octants; values in the tables for 25° and 35° are maximum values and only apply to octants with a 12.5° neutron pad extent.

6 3 Neutron Dosimetry

The passive neutron sensors included in the Braidwood Unit 1 surveillance program are listed in Table 6-6. Also given in Table 6-6 are the primary nuclear reactions and associated nuclear constants that were used in the evaluation of the neutron energy spectrum within the capsule and the subsequent determination of the various exposure parameters of interest [ϕ (E > 1.0 Mev), ϕ (E > 0.1 MeV), dpa].

The relative locations of the neutron sensors within the capsules are shown in Figure 4-2. The iron, nickel, copper, and cobalt-aluminum monitors, in wire form, were placed in holes drilled in spacers at several axial levels within the capsules. The cadmium-shielded neptunium and uranium fission monitors were accommodated within the dosimeter block located near the center of the capsule.

The use of passive monitors such as those listed in Table 6-6 does not yield a direct measure of the energy dependent flux level at the point of interest. Rather, the activation or fission process is a measure of the integrated effect that the time- and energy-dependent neutron flux has on the target material over the course of the irradiation period. An accurate assessment of the average neutron flux level incident on the various monitors may be derived from the activation measurements only if the irradiation parameters are well known. In particular, the following variables are of interest:

- The specific activity of each monitor.
- The operating history of the reactor.
- The energy response of the monitor.
- The neutron energy spectrum at the monitor location.
- The physical characteristics of the monitor.

The specific activity of each of the neutron monitors was determined using established ASTM procedures [15 through 28]. Following sample preparation and weighing, the activity of each monitor was determined by means of a lithium-drifted germanium, Ge(Li), gamma spectrometer. The irradiation history of the Braidwood Unit 1 reactor during cycle 1 was obtained from NUREG-0020, "Licensed Operating Reactors Status Summary Report" for the applicable period.

The irradiation history applicable to capsule U is given in Table 6-7. Measured and saturated reaction product specific activities as well as measured full power reaction rates are listed in Table 6-8. Reaction rate values were derived using the pertinent data from Tables 6-6 and 6-7.

The first term specifies purely random uncertainties while the second term describes short-range correlations over a range δ (Θ specifies the strength of the latter term.)

For the a priori calculated fluxes, a short-range correlation of $\delta = 6$ groups was used. This choice implies that neighboring groups are strongly correlated when Θ is close to 1. Strong long-range correlations (or anticorrelations) were justified based on information presented by R.E. Maerker [31]. Maerker's results are closely duplicated when $\delta = 6$. For the integral reaction rate covariances, simple normalization and random uncertainties were combined as deduced from experimental uncertainties.

Results of the FERRET evaluation of the capsule U dosimetry are given in Table 6-9. The data summarized in Table 6-9 indicated that the capsule received an integrated exposure of 3.79×10^{18} n/cm^2 (E > 1.0 MeV) with an associated uncertainty of ± 8%. Also reported are capsule exposures in terms of fluence (E > 0.1 MeV) and iron atom displacements (dpa). Summaries of the fit of the adjusted spectrum are provided in Table 6-10. In general, excellent results were achieved in the fits of the adjusted spectrum to the individual experimental reaction rates. The adjusted spectrum itself is tabulated in Table 6-11 for the FERRET 53 energy group structure.

A summary of the measured and calculated neutron exposure of capsule U is presented in Table 6-12. The agreement between calculation and measurement falls within ± 13% for all fast neutron exposure parameters listed. The thermal neutron exposure calculated for cycle 1 undepredicted the measured value by 62 percent.

Neutron exposure projections at key locations on the pressure vessel inner radius are given in Table 6-13. Along with the current (1.10 EFPY) exposure derived from the capsule U measurements, projections are also provided for an exposure period of 16 EFPY and to end of vessel design life (32 EFPY). The calculated design basis exposure rates given in Table 6-2 were used to perform projections beyond the end of cycle 1.

In the calculation of exposure gradients for use in the development of heatup and cooldown curves for the Braidwood Unit 1 reactor coolant system, exposure projections to 16 EFPY and 32 EFPY were employed. Data based on both a fluence (E > 1.0 MeV) slope and a plant specific dpa slope through the vessel wall are provided in Table 6-14. In order to access RT_{NDT} vs. fluence trend curves, dpa equivalent fast neutron fluence levels for the 1/4T and 3/4T positions were defined by the relations

$$\phi' \text{ (1/4T)} = \phi \text{ (Surface)} \left\{ \frac{\text{dpa (1/4T)}}{\text{dpa (Surface)}} \right\}$$

$$\phi' \text{ (3/4T)} = \phi \text{ (Surface)} \left\{ \frac{\text{dpa (3/4T)}}{\text{dpa (Surface)}} \right\}$$

Using this approach results in the dpa equivalent fluence values listed in Table 6-14.

In Table 6-15 updated lead factors are listed for each of the Braidwood Unit 1 surveillance capsules. These data may be used as a guide in establishing future withdrawal schedules for the remaining capsules.

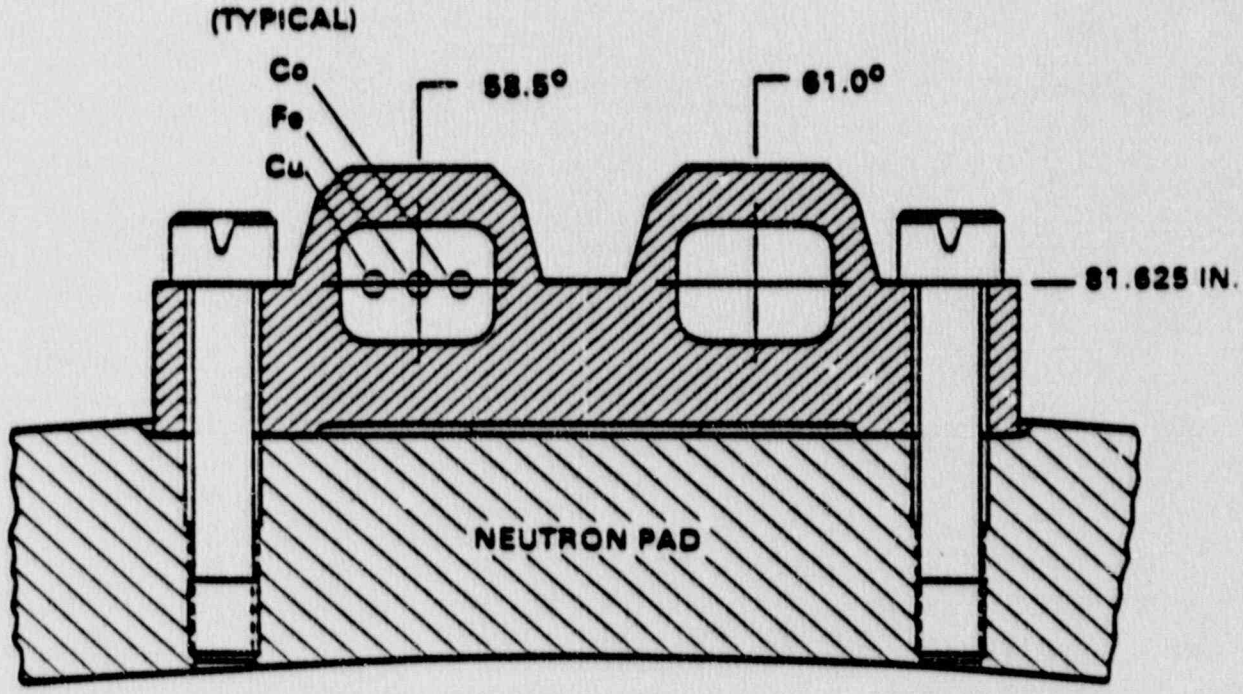

Figure 6-1. Plan View of a Dual Reactor Vessel Surveillance Capsule

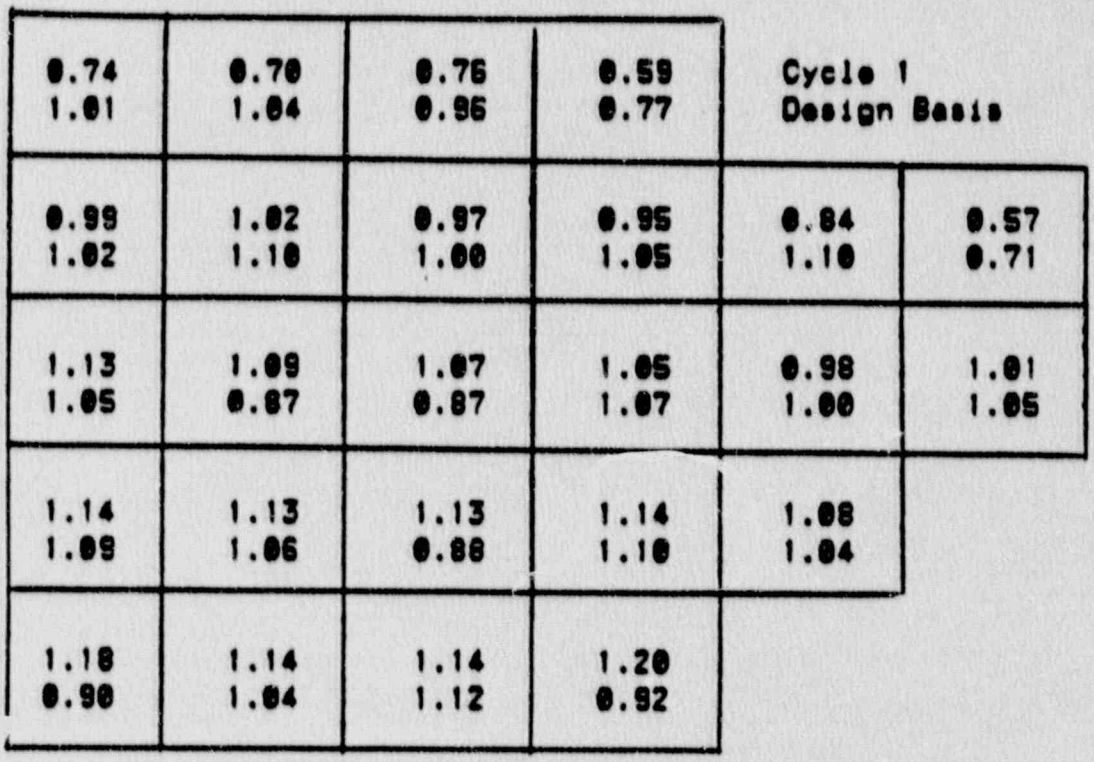

Figure 6-2. Core Power Distributions Used in Transport Calculations for Braidwood Unit 1

TABLE 6-1

CALCULATED FAST NEUTRON EXPOSURE PARAMETERS

AT THE SURVEILLANCE CAPSULE CENTER

	DESIGN BASIS		CYCLE 1	
	29.0°	31.5°	29.0°	31.5°
ϕ (E > 1.0 MeV) (n/cm^2-sec)	1.13×10^{11}	1.21×10^{11}	8.84×10^{10}	9.51×10^{10}
ϕ (E > 0.1 MeV) (n/cm^2-sec)	5.07×10^{11}	5.44×10^{11}	3.97×10^{11}	4.28×10^{11}
dpa/sec	2.21×10^{-10}	2.37×10^{-10}	1.73×10^{-10}	1.86×10^{-10}

TABLE 6-2

CALCULATED FAST NEUTRON EXPOSURE PARAMETERS AT
THE PRESSURE VESSEL CLAD/BASE METAL INTERFACE

DESIGN BASIS

	0°	15°	25°	35°	45°
ϕ(E> 1.0Mev) (n/cm^2-sec)	1.78×10^{10}	2.66×10^{10}	3.01×10^{10}	2.45×10^{10}	2.81×10^{10}
ϕ(E> 0.1Mev) (n/cm^2-sec)	3.70×10^{10}	5.60×10^{10}	8.22×10^{10}	6.96×10^{10}	7.04×10^{10}
dpa/sec	2.77×10^{-11}	4.12×10^{-11}	5.04×10^{-11}	4.15×10^{-11}	4.48×10^{-11}

CYCLE 1 SPECIFIC

	0°	15°	25°	35°	45°
ϕ(E> 1.0Mev) (n/cm^2-sec)	1.32×10^{10}	2.06×10^{10}	2.38×10^{10}	1.98×10^{10}	2.31×10^{10}
ϕ(E> 0.1Mev) (n/cm^2-sec)	2.74×10^{10}	4.34×10^{10}	6.50×10^{10}	5.62×10^{10}	5.79×10^{10}
dpa/sec	2.05×10^{-11}	3.19×10^{-11}	3.99×10^{-11}	3.35×10^{-11}	3.68×10^{-11}

TABLE 6-3
RELATIVE RADIAL DISTRIBUTIONS OF NEUTRON FLUX (E > 1.0 MeV)
WITHIN THE PRESSURE VESSEL WALL

Radius (cm)	0°	15°	25°	35°	45°
220.27[1]	1.00	1.00	1.00	1.00	1.00
220.64	0.976	0.979	0.980	0.977	0.979
221.66	0.888	0.891	0.893	0.891	0.889
222.99	0.768	0.770	0.772	0.770	0.766
224.31	0.653	0.653	0.657	0.655	0.648
225.63	0.551	0.550	0.554	0.552	0.543
226.95	0.462	0.460	0.465	0.463	0.452
228.28	0.386	0.384	0.388	0.386	0.375
229.60	0.321	0.319	0.324	0.321	0.311
230.92	0.267	0.265	0.271	0.267	0.257
232.25	0.221	0.219	0.223	0.221	0.211
233.57	0.183	0.181	0.185	0.183	0.174
234.89	0.151	0.149	0.153	0.151	0.142
236.22	0.124	0.122	0.126	0.124	0.116
237.54	0.102	0.100	0.104	0.102	0.0945
238.86	0.0828	0.0817	0.0846	0.0835	0.0762
240.19	0.0671	0.0660	0.0689	0.0679	0.0608
241.51	0.0538	0.0522	0.0550	0.0545	0.0471
242.17[2]	0.0506	0.0488	0.0518	0.0521	0.0438

NOTES: 1) Base Metal Inner Radius
2) Base Metal Outer Radius

TABLE 6-4

RELATIVE RADIAL DISTRIBUTIONS OF NEUTRON FLUX (E > 0.1 MeV)
WITHIN THE PRESSURE VESSEL WALL

Radius (cm)	0°	15°	25°	35°	45°
220.27[1]	1.00	1.00	1.00	1.00	1.00
220.64	1.00	1.00	1.00	1.00	1.00
221.66	1.00	1.00	1.00	0.999	0.995
222.99	0.974	0.969	0.974	0.959	0.956
224.31	0.927	0.920	0.927	0.907	0.901
225.63	0.874	0.865	0.874	0.850	0.842
226.95	0.818	0.808	0.818	0.792	0.782
228.28	0.761	0.750	0.716	0.734	0.721
229.60	0.705	0.693	0.704	0.677	0.662
230.92	0.649	0.637	0.649	0.621	0.605
232.25	0.594	0.582	0.594	0.567	0.549
233.57	0.540	0.529	0.542	0.515	0.495
234.89	0.487	0.478	0.490	0.465	0.443
236.22	0.436	0.428	0.440	0.416	0.392
237.54	0.386	0.380	0.392	0.369	0.343
238.86	0.337	0.333	0.344	0.324	0.295
240.19	0.289	0.287	0.298	0.279	0.248
241.51	0.244	0.238	0.249	0.233	0.201
242.17[2]	0.233	0.226	0.237	0.223	0.188

NOTES: 1) Base Metal Inner Radius
2) Base Metal Outer Radius

TABLE 6-5

RELATIVE RADIAL DISTRIBUTIONS OF IRON DISPLACEMENT RATE (dpa)
WITHIN THE PRESSURE VESSEL WALL

Radius (cm)	0°	15°	25°	35°	45°
220.27[1]	1.00	1.00	1.00	1.00	1.00
220.64	0.984	0.981	0.984	0.983	0.984
221.66	0.912	0.909	0.917	0.921	0.915
222.99	0.815	0.812	0.826	0.833	0.821
224.31	0.722	0.719	0.737	0.747	0.730
225.63	0.638	0.634	0.656	0.668	0.647
226.95	0.563	0.559	0.584	0.597	0.572
228.28	0.497	0.493	0.519	0.533	0.506
229.60	0.439	0.435	0.462	0.475	0.447
230.92	0.387	0.383	0.410	0.423	0.394
232.25	0.341	0.338	0.364	0.376	0.347
233.57	0.300	0.297	0.322	0.334	0.305
234.89	0.263	0.261	0.285	0.295	0.266
236.22	0.230	0.228	0.250	0.260	0.231
237.54	0.199	0.198	0.218	0.227	0.199
238.86	0.171	0.170	0.189	0.196	0.169
240.19	0.145	0.144	0.161	0.167	0.140
241.51	0.121	0.119	0.135	0.139	0.113
242.17[2]	0.116	0.113	0.128	0.134	0.106

NOTES: 1) Base Metal Inner Radius
2) Base Metal Outer Radius

TABLE 6-6

NUCLEAR PARAMETERS FOR NEUTRON FLUX MONITORS

Monitor Material	Reaction of Interest	Target Weight Fraction	Response Range	Product Half-Life	Fission Yield (%)
Copper	$Cu^{63}(n,\alpha)Co^{60}$	0.6917	E > 4.7 MeV	5.272 yrs	
Iron	$Fe^{54}(n,p)Mn^{54}$	0.0582	E > 1.0 MeV	312.2 days	
Nickel	$Ni^{58}(n,p)Co^{58}$	0.6830	E > 1.0 MeV	70.90 days	
Uranium-238*	$U^{238}(n,f)Cs^{137}$	1.0	E > 0.4 MeV	30.12 yrs	5.99
Neptunium-237*	$Np^{237}(n,f)Cs^{137}$	1.0	E > 0.08 MeV	30.12 yrs	6.50
Cobalt-Aluminum*	$Co^{59}(n,\gamma)Co^{60}$	0.0015	0.4ev>E> 0.015 MeV	5.272 yrs	
Cobalt-Aluminum	$Co^{59}(n,\gamma)Co^{60}$	0.0015	E > 0.015 MeV	5.272 yrs	

*Denotes that monitor is cadmium shielded.

TABLE 6-7

IRRADIATION HISTORY OF NEUTRON SENSORS
CONTAINED IN CAPSULE U

Irradiation Period	P_j (MW_t)	$\frac{P_j}{P_{Ref.}}$	Irradiation Time (days)	Decay Time (days)
7/87	134	.039	20	1035
8/87	286	.084	31	1004
9/87	568	.167	30	974
10/87	1255	.368	31	943
11/87	2084	.611	30	913
12/87	2548	.747	31	882
1/88	64	.019	31	851
2/88	0	.000	29	822
3/88	66	.019	31	791
4/88	215	.063	30	761
5/88	2203	.646	31	730
6/88	2351	.689	30	700
7/88	246	.072	31	669
8/88	2920	.856	31	638
9/88	2401	.704	30	608
10/88	2704	.793	31	577
11/88	2703	.792	30	547
12/88	3129	.917	31	516
1/89	1836	.538	31	485
2/89	2764	.810	28	457
3/89	2795	.819	31	426
4/89	1773	.520	30	396
5/89	2872	.842	31	365
6/89	2967	.870	30	335
7/89	2252	.660	31	304
8/89	1851	.543	31	273
9/89	757	.222	2	271

NOTE: Reference Power = 3411 MW_t

TABLE 6-8

MEASURED SENSOR ACTIVITIES AND REACTION RATES

Monitor and Axial Location	Measured Activity (dis/sec-gm)	Saturated Activity (dis/sec-gm)	Reaction Rate (RPS/NUCLEUS)
Cu-63 (n,α) Co-60			
Top	5.16×10^{4}	4.38×10^{5}	
Middle	4.53×10^{4}	3.84×10^{5}	
Bottom	4.50×10^{4}	3.82×10^{5}	
Average	4.73×10^{4}	4.01×10^{5}	6.12×10^{-17}
Fe-54(n,p) Mn-54			
Top	1.08×10^{6}	3.98×10^{6}	
Middle	9.89×10^{5}	3.65×10^{6}	
Bottom	9.74×10^{5}	3.59×10^{6}	
Average	1.01×10^{6}	3.74×10^{6}	5.96×10^{-15}
Ni-58 (n,p) Co-58			
Top	2.65×10^{6}	5.56×10^{7}	
Middle	2.43×10^{6}	5.10×10^{7}	
Bottom	2.42×10^{6}	5.08×10^{7}	
Average	2.50×10^{6}	5.25×10^{7}	7.49×10^{-15}
U-238 (n,f) Cs-137 (Cd)			
Middle	1.33×10^{5}	5.46×10^{6}	3.60×10^{-14}

TABLE 6-8

MEASURED SENSOR ACTIVITIES AND REACTION RATES - cont'd

Monitor and Axial Location	Measured Activity (dis/sec-gm)	Saturated Activity (dis/sec-gm)	Reaction Rate (RPS/NUCLEUS)
Np-237(n,f) Cs-137 (Cd)			
Middle	1.32×10^{6}	5.41×10^{7}	3.28×10^{-13}
Co-59 (n,γ) Co-60			
Top	1.06×10^{7}	8.95×10^{7}	
Middle	1.06×10^{7}	8.99×10^{7}	
Bottom	1.06×10^{7}	8.99×10^{7}	
Average	1.06×10^{7}	8.98×10^{7}	5.86×10^{-12}
Co-59 (n,γ) Co-60 (Cd)			
Bottom	5.43×10^{6}	4.61×10^{7}	
Average	5.43×10^{6}	4.61×10^{7}	3.01×10^{-12}

TABLE 6-9

SUMMARY OF NEUTRON DOSIMETRY RESULTS

	TIME AVERAGED EXPOSURE RATES	
ϕ (E> 1.0 MeV) {n/cm^2-sec}	1.09×10^{11}	± 8%
ϕ (E> 0.1 MeV) {n/cm^2-sec}	4.80×10^{11}	± 15%
dpa/sec	2.09×10^{-10}	± 11%
ϕ(E< 0.414 eV) {n/cm^2-sec}	1.17×10^{11}	± 21%
	INTEGRATED CAPSULE EXPOSURE	
Φ (E> 1.0 MeV) {n/cm^2}	3.79×10^{18}	± 8%
Φ (E> 0.1 MeV) {n/cm^2}	1.67×10^{19}	± 15%
dpa	7.26×10^{-3}	± 11%
Φ (E< 0.414 eV) {n/cm^2}	4.06×10^{18}	± 21%

NOTE: Total Irradiation Time = 1.10 EFPY

TABLE 6-10

COMPARISON OF MEASURED AND FERRET CALCULATED
REACTION RATES AT THE SURVEILLANCE CAPSULE CENTER

Reaction	Measured	Adjusted Calculation	C/M
Cu-63 (n,α) Co-60	6.12×10^{-17}	6.19×10^{-17}	1.01
Fe-54 (n,p) Mn-54	5.96×10^{-15}	5.85×10^{-15}	0.98
Ni-58 (n,p) Co-58	7.49×10^{-15}	7.66×10^{-15}	1.02
U-238 (n,f) Cs-137 (Cd)	3.60×10^{-14}	3.35×10^{-14}	0.93
Np-237 (n,f) Cs-137 (Cd)	3.28×10^{-13}	3.37×10^{-13}	1.03
Co-59 (n,γ) Co-60 (Cd)	3.01×10^{-12}	3.02×10^{-12}	0.99
Co-59 (n,γ) Co-60	5.86×10^{-12}	5.81×10^{-12}	1.00

TABLE 6-11

ADJUSTED NEUTRON ENERGY SPECTRUM AT

THE SURVEILLANCE CAPSULE CENTER

Group	Energy (Mev)	Adjusted Flux (n/cm2-sec)	Group	Energy (Mev)	Adjusted Flux (n/cm2-sec)
1	1.73×10^{1}	8.93×10^{6}	28	9.12×10^{-3}	2.24×10^{10}
2	1.49×10^{1}	2.01×10^{7}	29	5.53×10^{-3}	2.90×10^{10}
3	1.35×10^{1}	7.72×10^{7}	30	3.36×10^{-3}	9.06×10^{9}
4	1.16×10^{1}	1.72×10^{8}	31	2.84×10^{-3}	8.67×10^{9}
5	1.00×10^{1}	3.75×10^{8}	32	2.40×10^{-3}	8.36×10^{9}
6	8.61×10^{0}	6.35×10^{8}	33	2.04×10^{-3}	2.36×10^{10}
7	7.41×10^{0}	1.44×10^{9}	34	1.23×10^{-3}	2.18×10^{10}
8	6.07×10^{0}	2.04×10^{9}	35	7.49×10^{-4}	2.02×10^{10}
9	4.97×10^{0}	4.28×10^{9}	36	4.54×10^{-4}	1.93×10^{10}
10	3.68×10^{0}	5.67×10^{9}	37	2.75×10^{-4}	2.08×10^{10}
11	2.87×10^{0}	1.19×10^{10}	38	1.67×10^{-4}	2.25×10^{10}
12	2.23×10^{0}	1.65×10^{10}	39	1.01×10^{-4}	2.25×10^{10}
13	1.74×10^{0}	2.33×10^{10}	40	6.14×10^{-5}	2.23×10^{10}
14	1.35×10^{0}	2.60×10^{10}	41	3.73×10^{-5}	2.18×10^{10}
15	1.11×10^{0}	4.76×10^{10}	42	2.26×10^{-5}	2.11×10^{10}
16	8.21×10^{-1}	5.45×10^{10}	43	1.37×10^{-5}	2.05×10^{10}
17	6.39×10^{-1}	5.68×10^{10}	44	8.32×10^{-6}	1.95×10^{10}
18	4.98×10^{-1}	4.13×10^{10}	45	5.04×10^{-6}	1.80×10^{10}
19	3.88×10^{-1}	5.81×10^{10}	46	3.06×10^{-6}	1.68×10^{10}
20	3.02×10^{-1}	5.99×10^{10}	47	1.86×10^{-6}	1.55×10^{10}
21	1.83×10^{-1}	5.94×10^{10}	48	1.13×10^{-6}	1.15×10^{10}
22	1.11×10^{-1}	4.76×10^{10}	49	6.83×10^{-7}	1.48×10^{10}
23	6.74×10^{-2}	3.31×10^{10}	50	4.14×10^{-7}	1.98×10^{10}
24	4.09×10^{-2}	1.88×10^{10}	51	2.51×10^{-7}	1.99×10^{9}
25	2.55×10^{-2}	2.47×10^{10}	52	1.52×10^{-7}	1.91×10^{9}
26	1.99×10^{-2}	1.22×10^{10}	53	9.24×10^{-8}	5.85×10^{10}
27	1.50×10^{-2}	1.55×10^{10}			

NOTE: Tabulated energy levels represent the upper energy of each group.

TABLE 6-12

COMPARISON OF CALCULATED AND MEASURED
EXPOSURE LEVELS FOR CAPSULE U

	Calculated	Measured	C/M
Φ(E> 1.0 MeV) {n/cm^2}	3.30 x 10^{18}	3.79 x 10^{18}	0.87
Φ(E> 0.1 MeV) {n/cm^2}	1.49 x 10^{19}	1.67 x 10^{19}	0.89
dpa	6.46 x 10^{-3}	7.26 x 10^{-3}	0.89
Φ(E< 0.414 eV) {n/cm^2}	1.57 x 10^{18}	4.06 x 10^{18}	0.39

TABLE 6-13

NEUTRON EXPOSURE PROJECTIONS AT KEY LOCATIONS

ON THE PRESSURE VESSEL CLAD/BASE METAL INTERFACE FOR BRAIDWOOD UNIT 1

	AZIMUTHAL ANGLE				
	0°	15°	25°(a)	35°	45°
1.10 EFPY					
Φ(E< 1.0 MeV) (n/cm^2)	5.27×10^{17}	8.22×10^{17}	9.50×10^{17}	7.90×10^{17}	9.22×10^{17}
Φ(E> 0.1 MeV) (n/cm^2)	1.07×10^{18}	1.69×10^{18}	2.54×10^{18}	2.19×10^{18}	2.26×10^{18}
dpa	8.00×10^{-4}	1.24×10^{-3}	1.56×10^{-3}	1.31×10^{-3}	1.44×10^{-3}
16.0 EFPY					
Φ(E> 1.0 MeV) (n/cm^2)	8.90×10^{18}	1.33×10^{19}	1.51×10^{19}	1.23×10^{19}	1.41×10^{19}
Φ(E> 0.1 MeV) (n/cm^2)	1.84×10^{19}	2.80×10^{19}	4.11×10^{19}	3.48×10^{19}	3.53×10^{19}
dpa	1.38×10^{-2}	2.06×10^{-2}	2.52×10^{-2}	2.08×10^{-2}	2.25×10^{-2}
32.0 EFPY					
Φ(E> 1.0 MeV) (n/cm^2)	1.79×10^{19}	2.68×10^{19}	3.03×10^{19}	2.47×10^{19}	2.83×10^{19}
Φ(E> 0.1 MeV) (n/cm^2)	3.71×10^{19}	5.62×10^{19}	8.26×10^{19}	7.00×10^{19}	7.08×10^{19}
dpa	2.78×10^{-2}	4.14×10^{-2}	5.07×10^{-2}	4.17×10^{-2}	4.51×10^{-2}

(a) Maximum point on the pressure vessel

TABLE 6-14

NEUTRON EXPOSURE VALUES FOR USE IN THE GENERATION OF HEATUP/COOLDOWN CURVES

16 EFPY

	NEUTRON FLUENCE (E> 1.0 MeV) SLOPE (n/cm^2)			dpa SLOPE (equivalent n/cm^2)		
	Surface	1/4 T	3/4 T	Surface	1/4 T	3/4 T
0°	8.90×10^{18}	4.83×10^{18}	1.03×10^{18}	8.90×10^{18}	5.61×10^{18}	1.95×10^{18}
15°	1.33×10^{19}	7.20×10^{18}	1.51×10^{18}	1.33×10^{19}	8.34×10^{18}	2.88×10^{18}
25°(a)	1.51×10^{19}	8.24×10^{18}	1.78×10^{18}	1.51×10^{19}	9.80×10^{18}	3.59×10^{18}
35°	1.23×10^{19}	6.69×10^{18}	1.43×10^{18}	1.23×10^{19}	8.15×10^{18}	3.05×10^{18}
45°	1.41×10^{19}	7.54×10^{18}	1.52×10^{18}	1.41×10^{19}	9.02×10^{18}	3.09×10^{18}

32 EFPY

	NEUTRON FLUENCE (E> 1.0 MeV) SLOPE (n/cm^2)			dpa SLOPE (equivalent n/cm^2)		
	Surface	1/4 T	3/4 T	Surface	1/4 T	3/4 T
0°	1.79×10^{19}	9.72×10^{18}	2.07×10^{18}	1.79×10^{19}	1.13×10^{19}	3.92×10^{18}
15°	2.68×10^{19}	1.45×10^{19}	3.05×10^{18}	2.68×10^{19}	1.69×10^{19}	5.81×10^{18}
25°(a)	3.03×10^{19}	1.66×10^{19}	3.57×10^{18}	3.03×10^{19}	1.97×10^{19}	7.21×10^{18}
35°	2.47×10^{19}	1.35×10^{19}	2.86×10^{18}	2.47×10^{19}	1.64×10^{19}	6.12×10^{18}
45°	2.83×10^{19}	1.52×10^{19}	3.06×10^{18}	2.83×10^{19}	1.81×10^{19}	6.20×10^{18}

(a) Maximum point on the pressure vessel

TABLE 6-15

UPDATED LEAD FACTORS FOR BRAIDWOOD UNIT 1
SURVEILLANCE CAPSULES

Capsule	Lead Factor
U	4.00[(a)]
X	4.02
W	4.02
Z	4.02
V	3.75
Y	3.75

(a) Plant specific evaluation

SECTION 7.0
SURVEILLANCE CAPSULE REMOVAL SCHEDULE

The removal schedule listed below was projected based on the calculated design basis neutron flux levels given in Table 6-1. If the plant operates with a low leakage fuel management strategy, the neutron flux at the vessel wall and the capsule locations would be reduced. Thus, the fluence levels reached at the target EFPY's would be correspondingly decreased.

For plants similar in design to Braidwood Unit 1, operation with low leakage fuel management typically results in neutron fluence rates at the capsule locations of approximately $2.7X10^{18}$ n/cm^2-EFPY and $3.0X10^{18}$ n/cm^2-EFPY at the 29° and 31.5° capsule locations, respectively. These values can be used to readjust withdrawal schedules to accommodate low leakage operation.

The following removal schedule meets ASTM E185-82, is based on the design base fluence calculations and is recommended for future capsules to be removed from the Braidwood Unit 1 reactor vessel:

Capsule	Location (deg.)	Capsule Lead Factor	Removal Time (b)	Estimated Fluence (n/cm^2)
U	58.5	4.00	1.10 (Removed)(a)	3.79×10^{18}
X	238.5	4.02	4.5	1.7×10^{19}(c)
V	61.0	3.75	9.0	3.2×10^{19}(d)
Y	241.0	3.75	15	5.3×10^{19}
W	121.5	4.02	Standby	-
Z	301.5	4.02	Standby	-

(a) Plant Specific Evaluation
(b) Effective full power years from plant startup.
(c) Approximate fluence at 1/4 thickness reactor vessel wall at end of life (32 EFPY).
(d) Approximate fluence at reactor vessel inner wall at end of life (32 EFPY).

SECTION 8.0
REFERENCES

1. Yanichko and Singer, "Commonwealth Edison Company Braidwood Station Unit No. 1, Reactor Vessel Radiation Surveillance Program," WCAP-9807, February 1981.

2. Code of Federal Regulations, 10CFR50, Appendix G, "Fracture Toughness Requirements", and Appendix H, "Reactor Vessel Material Surveillance Program Requirements," U.S. Nuclear Regulatory Commission, Washington, D. C.

3. Regulatory Guide 1.99, Proposed Revision 2, "Radiation Damage to Reactor Vessel Materials", U.S. Nuclear Regulatory Commission, February, 1986.

4. Section III of the ASME Boiler and Pressure Vessel Code, Appendix G, "Protection Against Nonductile Failure."

5. ASTM E208, "Standard Test Method for Conducting Drop-Weight Test to Determine Nil-Ductility Transition Temperature of Ferritic Steels."

6. ASTM E 185-82, "Standard Practice for Light-Water Cooled Nuclear Power Reactor Vessels, E 706 (IF)."

7. ASTM E 23-88, "Standard Test Methods for Notched Bar Impact Testing of Metallic Materials."

8. ASTM A 370-89, "Standard Test Methods and Definitions for Mechanical Testing of Steel Products."

9. ASTM E 8-89, "Standard Test Methods of Tension Testing of Metallic Materials."

10. ASTM E 21-79, "Standard Practice for Elevated Temperature Tension Tests of Metallic Materials."

11. ASTM E 83-85, "Standard Practice for Verification and Classification of Extensometers."

12. R. G. Soltesz, R. K. Disney, J. Jedruch, and S. L. Ziegler, "Nuclear Rocket Shielding Methods, Modification, Updating and Input Data Preparation. Vol. 5--Two-Dimensional Discrete Ordinates Transport Technique", WANL-PR(LL)-034, Vol. 5, August 1970.

13. "ORNL RSCI Data Library Collection DLC-76 SAILOR Coupled Self-Shielded, 47 Neutron, 20 Gamma-Ray, P3, Cross Section Library for Light Water Reactors".

14. J. V. Alexander, et. al., "Core Physics Parameters and Plant Operations Data for the Braidwood Generating Station Unit 1 Cycle 1", WCAP-10935, June 1986. (Proprietary)

15. ASTM Designation E482-82, "Standard Guide for Application of Neutron Transport Methods for Reactor Vessel Surveillance", in ASTM Standards, Section 12, American Society for Testing and Materials, Philadelphia, PA, 1984.

16. ASTM Designation E560-77, "Standard Recommended Practice for Extrapolating Reactor Vessel Surveillance Dosimetry Results", in ASTM Standards, Section 12, American Society for Testing and Materials, Philadelphia, PA, 1984.

17. ASTM Designation E693-79, "Standard Practice for Characterizing Neutron Exposures in Ferritic Steels in Terms of Displacements per Atom (dpa)", in ASTM Standards, Section 12, American Society for Testing and Materials, Philadelphia, PA, 1984.

18. ASTM Designation E706-81a, "Standard Master Matrix for Light-Water Reactor Pressure Vessel Surveillance Standard", in ASTM Standards, Section 12, American Society for Testing and Materials, Philadelphia, PA, 1984.

19. ASTM Designation E853-84, "Standard Practice for Analysis and Interpretation of Light-Water Reactor Surveillance Results", in ASTM Standards, Section 12, American Society for Testing and Materials, Philadelphia, PA, 1984.

20. ASTM Designation E261-77, "Standard Method for Determining Neutron Flux, Fluence, and Spectra by Radioactivation Techniques", in ASTM Standards, Section 12, American Society for Testing and Materials, Philadelphia, PA, 1984.

21. ASTM Designation E262-77, "Standard Method for Measuring Thermal Neutron Flux by Radioactivation Techniques", in ASTM Standards, Section 12, American Society for Testing and Materials, Philadelphia, PA, 1984.

22. ASTM Designation E263-82, "Standard Method for Determining Fast-Neutron Flux Density by Radioactivation of Iron", in ASTM Standards, Section 12, American Society for Testing and Materials, Philadelphia, PA, 1984.

23. ASTM Designation E264-82, "Standard Method for Determining Fast-Neutron Flux Density by Radioactivation of Nickel", in ASTM Standards, Section 12, American Society for Testing and Materials, Philadelphia, PA, 1984.

24. ASTM Designation E481-78, "Standard Method for Measuring Neutron-Flux Density by Radioactivation of Cobalt and Silver", in ASTM Standards, Section 12, American Society for Testing and Materials, Philadelphia, PA, 1984.

25. ASTM Designation E523-82, "Standard Method for Determining Fast-Neutron Flux Density by Radioactivation of Copper", in ASTM Standards, Section 12, American Society for Testing and Materials, Philadelphia, PA, 1984.

26. ASTM Designation E704-84, "Standard Method for Measuring Reaction Rates by Radioactivation of Uranium-238", in ASTM Standards, Section 12, American Society for Testing and Materials, Philadelphia, PA, 1984.

27. ASTM Designation E705-79, "Standard Method for Measuring Fast-Neutron Flux Density by Radioactivation of Neptunium-237", in ASTM Standards, Section 12, American Society for Testing and Materials, Philadelphia, PA, 1984.

28. ASTM Designation E1005-84, "Standard Method for Application and Analysis of Radiometric Monitors for Reactor Vessel Surveillance", in ASTM Standards, Section 12, American Society for Testing and Materials, Philadelphia, PA, 1984.

29. F. A. Schmittroth, FERRET Data Analysis Code, HEDL-TME 79-40, Hanford Engineering Development Laboratory, Richland, WA, September 1979.

30. W. N. McElroy, S. Berg and T. Crocket, A Computer-Automated Iterative Method of Neutron Flux Spectra Determined by Foil Activation, AFWL-TR-7-41, Vol. I-IV, Air Force Weapons Laboratory, Kirkland AFB, NM, July 1967.

31. EPRI-NP-2188, "Development and Demonstration of an Advanced Methodology for LWR Dosimetry Applications", R. E. Maerker, et al., 1981.